

Chapter 1

Exploring Quantum Hall Physics at Ultra-Low Temperatures and at High Pressures

Gábor A. Csáthy

*Department of Physics and Astronomy, Purdue University
525 Northwestern Avenue, West Lafayette, IN 47907
gcsathy@purdue.edu*

The use of ultra-low temperature cooling and of high hydrostatic pressure techniques has significantly expanded our understanding of the two-dimensional electron gas confined to GaAs/AlGaAs structures. This chapter reviews a selected set of experiments employing these specialized techniques in the study of the fractional quantum Hall states and of the charged ordered phases, such as the reentrant integer quantum Hall states and the quantum Hall nematic. Topics discussed include a successful cooling technique used, novel odd denominator fractional quantum Hall states, new transport results on even denominator fractional quantum Hall states and on reentrant integer quantum Hall states, and phase transitions observed in half-filled Landau levels.

1. Introduction

The two-dimensional electron gas (2DEG) is one of the richest model systems in condensed matter physics. Indeed, an impressive number of new phenomena were discovered in this system and several novel theoretical concepts were introduced to explain these phenomena. The integer¹ and fractional quantum Hall effect² are among the most important discoveries in the 2DEG and work on these Hall effects precipitated ideas on emergent quasiparticles³⁻⁷ and on topological concepts in condensed matter.^{8,9}

A large number of fractional quantum Hall states (FQHSs), especially the ones forming in the lowest Landau level, are well understood.^{10,11} Their properties are accounted for by Laughlin's wavefunction³ and Jain's theory of composite fermions.^{4,5} There are, however, a handful of fractional quantum Hall states which are thought to harbor more intricate topological order. These states, sometimes referred to as exotic fractional quantum Hall states,¹² remain in the focus of current interest.

Historically, the two most studied 2DEGs were confined to MOSFETs and GaAs/AlGaAs heterostructures.¹³ In addition to these two examples, 2DEGs are supported by various material hosts. Examples are AlAs/GaAlAs,¹⁴ CdTe/CdMgTe,¹⁵ Si/SiGe,¹⁶ Ge/SiGe,^{17,18} ZnO/MgZnO,¹⁹ hydrogen passivated

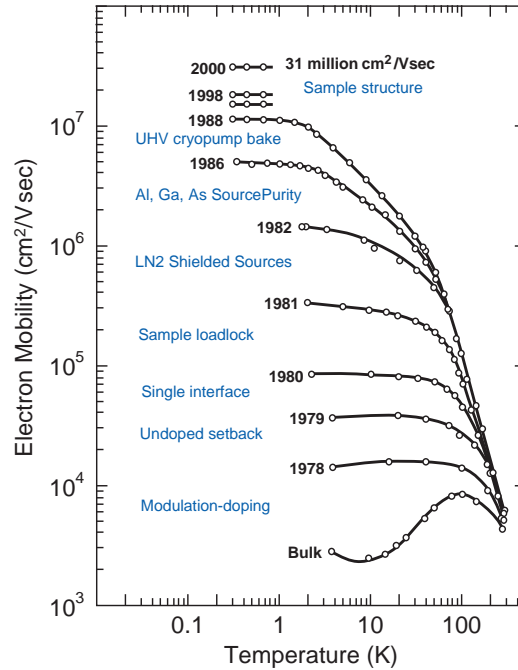


Fig. 1. Milestones in the evolution of the quality of 2DEGs in the GaAs/AlGaAs system, as measured by the electron mobility. Adapted from Ref.13.

Si surface,²⁰ and electrons on the surface of superfluid Helium.²¹ The study of the 2DEG enjoyed a resurgence of interest with pioneering work on graphene²² and other layered materials, such as transition metal dichalcogenides²³ and black phosphorus.²⁴ Work on the totality of 2DEGs highlighted some of the universal, host-independent physics. Examples are the formation of Landau levels in the integer quantum Hall regime and of composite fermions in the fractional quantum Hall regime. In addition, each of these hosts enriched the physics of the 2DEG. New physics resulted from 2DEGs with novel internal degrees of freedom, such as the valley and the pseudospin quantum number, and also from 2DEGs possessing an inherent anisotropy. Furthermore, the generation of Moiré lattices in layered van der Waals structures²⁵ led to Hofstadter physics²⁶ and, most recently, to magic angle superconductivity.²⁷

Even though 2DEGs confined to GaAs/AlGaAs heterostructures have been studied for more than three decades, this system continues to play a privileged role. A large number of phases were first seen in GaAs/AlGaAs. This is because numerous innovations in the Molecular Beam Epitaxy (MBE) growth technique culminated in 2DEGs of record high mobilities approaching 4×10^7 cm²/Vs or record long mean free paths in excess of 0.3 mm, when measured at temperatures below 1 Kelvin.¹³ Such high carrier mobilities are possible because of the exceedingly low defect levels

and also because of innovative sample structures. Growth efforts to further improve this material system continue.^{29–35} Historical milestones in the evolution of the GaAs MBE technology can be seen in Fig. 1.

One area in which 2DEGs in GaAs/AlGaAs excel when compared to those in other hosts is the support of both topological and traditional Landau phases. In contrast to topological phases, traditional Landau phases may be characterized by an order parameter. Charge ordered phases of the 2DEG are examples of such traditional Landau phases. The most well-known example of charge ordered phase is the Wigner crystal.³⁶ However, high quality 2DEGs allow for a more intricate charge ordering.^{37–39} The phase at half-filled Landau levels with a strong resistance anisotropy is commonly associated with the electronic nematic, whereas the so called reentrant integer quantum Hall states (RIQHSs) are thought to be identical to the electronic bubble phases.^{37–41} Recently an increasing amount of attention is lavished on the study of these charge ordered phases.

The 2DEG was probed with various ingenious techniques. However, electric transport played a special role among these techniques as it historically was used to reveal new electronic phases. Over the last decade or so, transport experiments performed at ultra-low temperature have been especially fertile in providing new insight into the physics of the 2DEG. In the following we present a personal view on some of these experiments, focusing mainly on the second Landau level of the 2DEG confined to GaAs/AlGaAs hosts. In Sec. 2 the reader will find experimental details of the ultra-low temperature cooling technique based on the He-3 immersion cell. Section 3 discusses recently discovered FQHSs, all of which are at odd denominators, followed by an examination of possible origins of these states. In Sec. 4 recent results of transport experiments on the even denominator FQHSs are discussed. Topics include phase transitions at the Landau level filling factor $\nu = 5/2$, a discussion of the energy gap of the FQHS at this filling factor, and its behavior in the presence of short-range alloy disorder. Section 5 contains results on RIQHSs in the second Landau level, such as magnetoresistive fingerprints of these states in high mobility samples, a discussion of the precursors of these states, and a summary of new, developing RIQHSs. Finally, the pressure-induced phase transition at $\nu = 5/2$ from a FQHS to the quantum Hall nematic is discussed in Sec. 6.

2. Cooling electrons below 10 mK and sample state preparation

Lowering the electronic temperature typically allows for the resolution of states of reduced energy scales. In other words, unless the energy spectrum is already disorder dominated, a lower temperature may reveal increasingly more fragile electronic ground states. Reducing the electron temperature, however, is not a trivial task. While modern dilution refrigerators routinely generate mixing chamber temperatures below 10 mK, similarly low electronic temperatures in semiconductor nanostructures are often difficult to achieve. This is because the combination of reduced electron-phonon coupling at milliKelvin temperatures and of minute amounts of

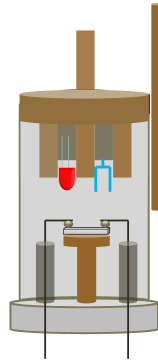


Fig. 2. Schematic of a He-3 immersion cell for ultra-low temperature transport measurements of 2DEGs. Adapted from Ref.55.

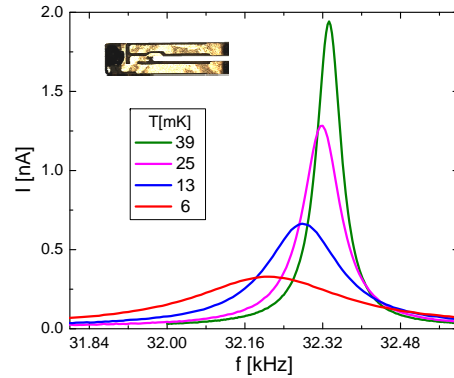


Fig. 3. A quartz tuning fork and the temperature dependence of its response when immersed into a He-3 bath. Adapted from Ref.55.

uncontrolled radiofrequency power traveling on the measurement wires; under such conditions the electron temperature in a transport setup is often higher than that of the phonons and also of the coldest spot of the refrigerator.

In this section we describe a successful electron thermalization setup based on a He-3 immersion cell. Such an immersion cell was first built by Jian-Sheng Xia and coauthors at the MicroKelvin Facility of the National High Magnetic Field Laboratory in Gainesville.⁴⁷ In this setup each ohmic contact of an electrically conductive sample, such as a 2DEG, is soldered onto individual wire heatsinks that consist of a silver wire surrounded by silver sinter. Constrained by the geometry of the superconductive magnet bore, one may achieve a surface area of the order of a m^2 for the sinter of each wire heatsink. In order to take advantage of such a large surface area for thermalization purposes, the 2DEG and the wire heatsinks are immersed into liquid He-3 that ensures both thermalization and electrical isolation. This thermalization setup was used to examine the quantization at $\nu = 5/2$,⁴⁴ to discover the $\nu = 12/5 = 2 + 2/5$ FQHS,⁴⁶ to study of metallic behavior in a hole gas,⁴⁸ and to understand the plateau-to-plateau transition in the integer quantum Hall regime.⁴⁹ A schematic of a He-3 immersion cell is shown in Fig. 2. Xia et al. have also built a He-3 immersion cell with a hydraulically driven rotator stage for tilted field measurements.⁵⁰ Since cooling electronic systems to ultra-low temperatures is increasingly important for the study of fragile electronic order, besides the immersion cell technology there are also efforts to develop alternative cooling techniques,^{51–54} some of which are designed on cryogen free platforms.

For our He-3 immersion cell we adopted the design from Ref.47. In contrast to the setup in Gainesville, instead of using a dilution refrigerator equipped with a nuclear demagnetization stage, we have attached our immersion cell to a modified dilution refrigerator with a 5 mK base temperature. Construction details can be

found in Ref.55. Microwave filters installed on measurement wires are a critical part of the setup. We used a three-stage filter on each wire. First, a set of capacitive filters mounted on the top of the refrigerator, as part of a D-sub connector, is used at room temperature. Second, on their way to the sample, the measurement wires are well heatsunk at each stage of the refrigerator and passed through silver epoxy embedded along about the one foot length of tail connecting the immersion cell to the mixing chamber. Finally, through the skin effect, silver sinters of each wire heatsink mounted within the immersion cell will also efficiently dissipate microwaves.⁵⁵ Additional low-pass RC filters with a cut-off frequency of 50 kHz and mounted on the still did not make a difference in electron thermalization, therefore they were later removed.

Parallel with the development of the cooling technology, there was also a flurry of activities in thermometry. Examples are thermometers based on resistive elements,⁵⁶ on Johnson noise measurements,^{57–59} and on measurement of the tunneling conductance.^{59–63} The extreme environment of temperatures below 10 mK and strong magnetic fields limit the choice of thermometers. The widely used RuO resistive sensors become unreliable for thermometry below about 20 mK, especially in strong fields. Paramagnetic susceptibility thermometers are not suitable for operation in strong magnetic fields. While He-3 melting curve thermometers could be used, we were deterred by the additional effort needed for handling the He-3 at high pressures. However, we already had liquid He-3 in the immersion cell for thermalization purposes, albeit the He-3 was not at the high pressures need for operation at the liquid-solid phase boundary required in a melting curve thermometer. Under such conditions the viscosity of the He-3 liquid provides a convenient way for temperature monitoring from about 100 mK down to the superfluid onset temperature (not within the reach of our instrument). Since viscosity is independent of the magnetic field, it is ideally suited for the demanding low temperature and strong magnetic field environment of measurements in the quantum Hall regime. We opted for a quartz tuning fork based viscometer.⁵⁵ An example of a quartz tuning fork and the temperature dependence of the response curve of the tuning fork immersed into liquid He-3 are shown Fig. 3.

Finally, the electronic state of 2DEGs confined to GaAs/AlGaAs is often prepared by a brief low temperature illumination using either a red light emitting diode facing the 2DEG^{64,65} or light guided towards the sample using fiber optics.⁶⁶ One effect of such illumination is the increase of the electron density that is desirable for robust ground states. In addition, illumination may also improve the homogeneity of the electron gas.

3. Recently discovered fractional quantum Hall states

In this section we discuss new FQHSs discovered in the 2DEG in the GaAs/AlGaAs system. Two of these, the FQHSs at $\nu = 2 + 6/13$ and at $\nu = 3 + 1/3$, were seen in the region of the second Landau level, whereas the FQHSs at $\nu = 4/11$ and

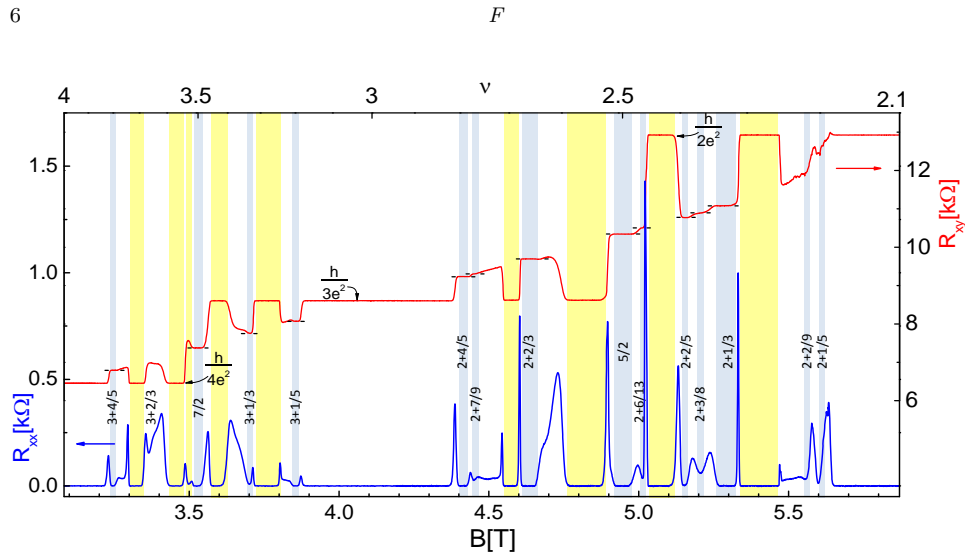


Fig. 4. A particularly rich magnetotransport trace measured at 6.9 mK in the second Landau level. Both spin branches are shown. Blue shades mark fractional quantum Hall states (FQHSs) at the labeled filling factors, whereas yellow shades show various reentrant integer quantum Hall states (RIQHSs). Adapted from Ref.71.

$\nu = 5/13$ develop in the lowest Landau level. These FQHSs are fragile, hence the use of the immersion cell technology played a central role in their discovery. We show that an analysis of the energy gaps reveals valuable insight into the nature of these FQHSs.

Ground states with a second Landau level character are the strongest in 2DEGs with the optimal electron density. Indeed, as a rule of thumb, the energy gap of a given FQHS increases with the value of the magnetic field at which it forms. Therefore in order to maximize the energy gap of a FQHS, one must use a 2DEG with the largest possible density. However, because the finite thickness of the electronic wavefunction in the direction perpendicular to the plane of the 2DEG, past a critical density the Fermi level moves to the lowest Landau level of the second electric subband. As shown by Shayegan and coauthors^{67,68} and also supported by theory,⁶⁹ such a population of the second electrical subband will have a strong influence on the ground states: the orbital part of the single particle wavefunction changes from a second Landau level character to a lowest Landau level character. The most dramatic consequence of populating the second electrical subband is the rapid collapse of the FQHS at $\nu = 5/2$ ^{67,68}. The optimal density is therefore the largest density at which the Fermi level falls into the second Landau level and at which ground states retain a second Landau level character. For a quantum well of a 30 nm width, the optimal density is about $3.0 \times 10^{11} \text{ cm}^{-2}$.

Fig. 4 shows magnetoresistance traces with a particularly rich structure over the full width of the second Landau level, i.e. both the lower and upper spin branches, in another 2DEG near its optimal density.^{70,71} FQHSs are shaded in blue, while RIQHSs in yellow. At first blush, magnetoresistance in the lower spin branch

of the second Landau level shown in Fig. 4 is similar to that in Ref.46. However, a more careful examination reveals a notable difference in the sharpness of several magnetoresistance peaks. For example, the width at half height of the peak in R_{xx} shown in Fig. 4 near $B = 5.02$ T is 6.6 mT, while of that near $B = 5.33$ T is merely 4.2 mT. In contrast, the corresponding peaks in Ref.46 are considerable wider. The differences in the two traces are surprising, given that samples and measurement conditions were comparable: the electron densities, mobilities, and the fridge temperatures were $n = 3.1 \times 10^{11} \text{ cm}^{-2}$, $\mu = 31 \times 10^6 \text{ cm}^2/\text{Vs}$, $T = 9 \text{ mK}$ in Ref.46, and $n = 3.0 \times 10^{11} \text{ cm}^{-2}$, $\mu = 32 \times 10^6 \text{ cm}^2/\text{Vs}$, $T = 6.9 \text{ mK}$ in Refs.70,71. The difference in the sharpness of the resistance peaks is likely attributed to a difference in sample homogeneity. Indeed, in the presence of a density variation, the magnetoresistance will be a convolution of magnetoresistances corresponding to the range of electron densities and therefore a density inhomogeneity will lead to a broadening of sharp resistive features. Density inhomogeneity in high quality GaAs/AlGaAs samples may be estimated from the widths of sharp magnetoresistance peaks,⁷² from an analysis of quantum lifetime measurements,⁷³ and it is also accessible with the micro-photoluminescence technique on lengthscales larger than the laser spotsize.^{74,75} We believe that the improved sample homogeneity results from a combination of improved sample growth and sample illumination techniques.

3.1. $\nu = 2 + 6/13$ and $\nu = 2 + 2/5$ fractional quantum Hall states

A particularly interesting region within the second Landau level is that of $2 + 1/3 < \nu < 2 + 2/3$, which was conjectured to host FQHSs with unusual topological order.⁷⁶ Several FQHSs in this region may have exotic fractional correlations.^{6,7,77-83} The FQHSs at the two endpoints of this range may be either Laughlin states or states radically different from it.⁸⁴⁻⁹² Until 2004, FQHSs in this region were detected, using a He-3 immersion cell, at $\nu = 5/2$, $\nu = 2 + 2/5$, and $\nu = 2 + 3/8$.⁴⁶ An account of FQHSs in GaAs/AlGaAs, including of the ones in the second Landau level, was published in 2008.⁹³

Another immersion cell experiment confirmed a fully quantized $\nu = 2 + 2/5$ FQHS, with an energy gap of 80 mK⁷⁰ in the $2 + 1/3 < \nu < 2 + 2/3$ range. It also yielded a new FQHS in this range at $\nu = 2 + 6/13$.⁷⁰ As seen in Fig.4, this FQHS is located between the $\nu = 5/2$ FQHS and a RIQHS. Since its first observation, the $\nu = 2 + 6/13$ FQHS has been seen in an increasing number of experiments.^{32,94-96}

The observation of a FQHS at $\nu = 2 + 6/13$ was a surprise. Indeed, Jain's model of non-interacting composite fermions⁴ offers a concise and elegant framework for the understanding of FQHSs developing at filling factors of the form $p/(2p \pm 1)$, with $p = 1, 2, 3, \dots$. One may notice that the subset of $\nu = 2 + 1/3$, $2 + 2/5$, and $2 + 6/13$ filling factors, at which there are FQHSs in the second Landau level, also belongs to the Jain sequence of the form $2 + p/(2p + 1)$, with $p = 1, 2$, and 6 , respectively. However, other FQHSs at intermediate values of $p = 3, 4$, and 5 are not present in Fig. 4. As shown in Fig. 5, the missing FQHSs are absent not only at the lowest

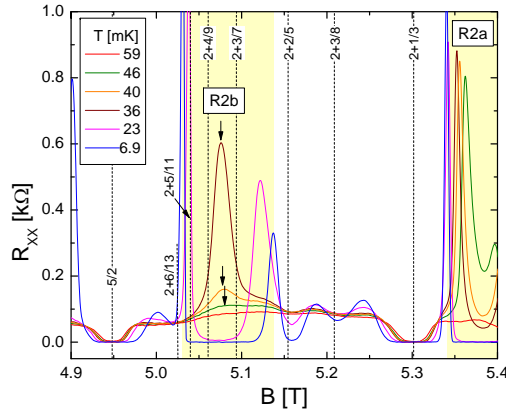


Fig. 5. Details of the temperature dependence of the magnetoresistance near the RIQHS $R2b$. Vertical arrows mark the precursor of the RIQHS $R2b$. Adapted from Ref.97.

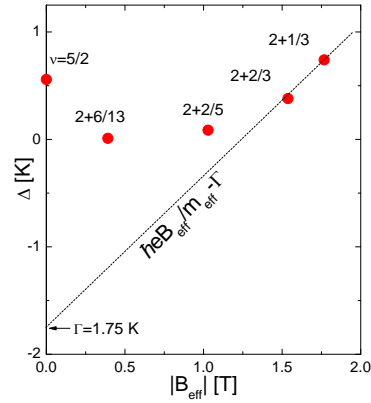


Fig. 6. Energy gaps of FQHSs in the $2 + 1/3 < \nu < 2 + 2/3$ range versus $|B_{eff}|$. Adapted from Ref.70.

temperatures, but for a range of temperatures.⁹⁷ Because of these absent FQHSs with $p = 3, 4$, and 5 , it was unexpected to see a FQHS of an unusually high order $p = 6$ at $\nu = 2 + 6/13$. We note that even though in other experiments local minima in R_{xx} were seen at $\nu = 2 + 4/9$ in Refs.31,98 and at $\nu = 2 + 3/7$ in Ref.98, in the absence of a Hall plateau the identification of a FQHS at these filling factors is inconclusive.^{31,98}

At this time it is not known why the $\nu = 2 + 3/7, 2 + 4/9$, and $2 + 5/11$ FQHSs are not present in Fig. 5. One explanation for the missing FQHSs at $\nu = 2 + 3/7, 2 + 4/9$, and $2 + 5/11$ may be offered by a competition with the RIQHS labeled $R2b$. If the energies of the competing RIQHS and FQHSs are comparable, one may expect incipient FQHSs near the onset temperature of the RIQHS. However, magnetotransport did not exhibit such features near the onset of the RIQHS $R2b$.⁹⁷ Indeed, gentle curvatures of the magnetoresistance seen in Fig. 5 near $\nu = 2 + 3/7$ and $2 + 4/9$ in traces measured at $T = 59, 46$, and 40 mK could not be assigned to incipient FQHSs; instead these features have been associated with magnetoresistive fingerprints of the precursor of the RIQHS.⁹⁷ This suggests that the RIQHS labeled $R2b$ is considerably more stable than the FQHSs and therefore it is strongly favored from an energetical point of view. According to a second argument presented in the following, if the FQHSs at $\nu = 2 + 2/5$ and $2 + 6/13$ have topological order different from that of the model of non-interaction composite fermions, then FQHSs at the intermediate filling factors $\nu = 2 + 3/7, 2 + 4/9$, and $2 + 5/11$ do not have to necessarily exist.

The development of FQHSs at filling factors belonging to the Jain sequence $2 + p/(2p + 1)$ does not necessarily mean that these FQHSs can be described by the model of non-interacting composite fermions. Indeed, there are ideas proposed

according to which in the presence of strong residual interactions between the composite fermions, the nature of a FQHS may be different from that predicted by the model of non-interacting composite fermions. An examination of the energy gaps of these FQHSs provided early insight in this regard.⁷⁰

In the following we discuss energy gaps of the odd denominator FQHSs of the second Landau level. We will use a widely used phenomenological model.^{99,100} The purpose of this model is to bridge the difference between energy gaps obtained from numerical experiments and those from measurements. The former are calculated in simulations that do not include any disorder, while the latter are extracted from measured data in real 2DEGs that necessarily have some disorder present. According to this simple model, the measured energy gap Δ is reduced from the expected theoretical value in the limit of no disorder, also called the intrinsic gap Δ^{int} , by an amount due to disorder broadening Γ :

$$\Delta = \Delta^{int} - \Gamma. \quad (1)$$

The intrinsic gap Δ^{int} contains effects of the finite width of the wavefunction in the direction perpendicular to the plane of the 2DEG and of Landau level mixing. Since disorder effects are not included into Δ^{int} , it may therefore be directly compared to gaps from numerical experiments, such the ones from exact diagonalization. Eq.(1) therefore offers a simple way to deal with the effects of the disorder on the energy gap, a task that remains challenging for the theory. The concept of disorder broadening was used to understand early gap measurements of FQHSs^{99,100} and also of the series of the FQHSs in the lowest Landau level.¹⁰¹ In the latter work, the dependence of gaps on the effective magnetic field was found linear. The slope of this linear dependence yields the cyclotron mass of the composite fermions.¹⁰¹ Furthermore, it was found that energy gaps extrapolate to a negative offset at zero effective magnetic field.¹⁰¹ This negative offset was identified with a filling factor independent Γ , with values between 1 and 2 K.

In the second Landau level the number of FQHSs is considerably less than that in the lowest Landau level. Nonetheless, as shown in Fig. 6, the simplest possible analysis involving a reflection of the FQHS at $\nu = 2 + 2/3$ to positive effective magnetic fields shows that a linear dependence of the gaps does no longer hold in the second Landau level.⁷⁰ The complex dependence of the energy gaps on the effective magnetic field indicates that residual interactions of the composite fermions are significant in the second Landau level and, as a result, at least some of the FQHSs may be beyond the model of non-interacting composite fermions.⁷⁰ If in addition the effective mass of composite fermions in the second Landau level is assumed to be the same as of those forming in the lowest Landau level, one finds that the energy gaps of the $\nu = 2 + 1/3$ and $2 + 2/3$ FQHSs are consistent with the model of free composite fermions when the disorder broadening is $\Gamma = 1.75$ K.⁷⁰ The expected energy gaps of FQHSs of free composite fermions under these assumptions are shown by a dashed line in Fig. 6. The proximity of the measured gaps at $\nu = 2 + 1/3$ and $2 + 2/3$ to the dashed line shown in Fig. 6 suggests that FQHSs at $\nu = 2 + 1/3$

and $2 + 2/3$ may be of the Laughlin type. Similar conclusions on the nature of the $\nu = 2 + 1/3$ and $2 + 2/3$ FQHSs were also drawn in studies of the neutral modes at $\nu = 2 + 1/3$ and $2 + 2/3$,¹⁰³ edge-to-edge tunneling experiments at $\nu = 2 + 2/3$,¹⁰⁴ and magnetoroton measurements at $\nu = 2 + 1/3$.¹⁰⁵ Nonetheless, overlap calculations of the numerically obtained wave function with the Laughlin state and other theory work suggests that the FQHS at $\nu = 2 + 1/3$ is not yet satisfactorily understood.^{84–92} The analysis presented above is the simplest possible one; an alternative model for the energy gaps at odd denominators may be found in Ref.102.

Under the assumptions described above, the measured energy gaps of both the $\nu = 2 + 6/13$ and $\nu = 2 + 2/5$ FQHSs are significantly larger than the expected values of a model of non-interacting composite fermions.⁷⁰ This discrepancy of the energy gaps, also shown in Fig. 6, constituted an early experimental evidence that the FQHSs at $\nu = 2 + 6/13$ and $2 + 2/5$ are not similar to their lowest Landau level counterparts forming at $\nu = 6/13$ and $2/5$, but they are likely of exotic, perhaps non-Abelian nature. The argument according to which the interactions between the composite fermions at $\nu = 2 + 6/13$ are significant enough to change the topological order of the FQHSs at this filling factor is not unreasonable, since similar interactions at the nearby filling factor $\nu = 5/2$ are known to drastically change the ground state from a Fermi sea of composite fermions to a FQHS. In fact the FQHSs at $\nu = 2 + 6/13$ and at $\nu = 5/2$ may be closely related. Indeed, according to a recent proposal, FQHSs at $\nu = 2 + 6/13$ and $\nu = 5/2$ as well as other FQHSs of the second Landau level may be accounted for within the same description based on parton wavefunctions.^{106–108}

The above analysis of the gaps has implications not only for the FQHS at $\nu = 2 + 6/13$, but also for the FQHS at $\nu = 2 + 2/5$. According to this analysis, the $\nu = 2 + 2/5$ FQHS is also an exotic FQHS.⁷⁰ Proposals for the description of the $\nu = 2 + 2/5$ FQHS include the Read-Rezayi parafermion construction,⁷ the particle-hole conjugate of this state,⁷⁸ the Bonderson-Slingerland state,⁷⁹ the Gaffnian,⁷⁷ the Levin-Halperin Abelian construction,⁸¹ multipartite composite fermion states,^{82,83} and a parton state.¹⁰⁸ Numerical work favors the Read-Rezayi description,^{7,109–112} which however is in close competition with the Bonderson-Slingerland state¹¹³. It appears that no single theory among the ones predicting exotic behavior at $\nu = 2 + 2/5$ and $2 + 6/13$ can account for FQHSs at these two filling factors in a natural way and therefore one may surmise that these two FQHSs have fundamentally different origins.

While at $\nu = 2 + 6/13$ there is a visible FQHS, a FQHS at the particle-hole symmetry related filling factor of $\nu = 2 + 7/13$ is conspicuously missing.⁷⁰ A similar lack of particle-hole symmetry is also observed at partial filling $2/5$. Indeed, as already discussed, the ground state at $\nu = 2 + 2/5$ is a FQHS, whereas at $\nu = 2 + 3/5$ a FQHS does not form. The lack of particle-hole symmetry at $\nu = 2 + 7/13$ and $\nu = 2 + 3/5$ affects FQHSs differently than the RIQHSs.⁹⁷ It is interesting to note that a related particle-hole asymmetry was also observed in a high quality bilayer

graphene.¹¹⁴ In this experiment a weak FQHS is seen at $\nu = 2 + 7/13$, but not at $\nu = 2 + 6/13$. However, in Ref.114 a competition with a RIQHS cannot be invoked. This result indicates that a particle-hole symmetry breaking effect, such as Landau level mixing, is likely at play and it favors one set of FQHSs, while suppresses fractional correlations at the particle-hole symmetric filling factor.

Finally, we note that data discussed above are all in the single layer limit, i.e. when the second electrical subband is not occupied. Recent work on the $\nu = 2 + 2/5$ and $2 + 3/5$ FQHSs in a wide quantum well in a GaAs/AlGaAs system in which the second subband is occupied suggests that these two FQHSs belong to the model of non-interacting composite fermions.⁶⁷ Once the orbital wavefunctions acquire a lowest Landau level character in samples with the second electrical subband occupied, particle-hole symmetry of the FQHSs appears to be restored.⁶⁷

3.2. $\nu = 3 + 1/3$ fractional quantum Hall state

The upper spin branch of the second Landau level, i.e. the $3 < \nu < 4$ region, is at a lower magnetic fields and therefore hosts fewer FQHSs than the lower spin branch. Early work on this region established the FQHSs at $\nu = 7/2$, $\nu = 3 + 1/5$, and $\nu = 3 + 4/5$ as well as four RIQHSs.⁴⁵ The FQHS discovered at $\nu = 3 + 1/3$ is the most recently seen ground state in this region.⁷¹ A FQHS at this filling factor is identified by a vanishing magnetoresistance and a Hall resistance quantized to $h/(3 + 1/3)e^2$.

Even though in Fig.4 a distinct minimum in the magnetoresistance is also observed at $\nu = 3 + 2/3$, a FQHS at this filling factor is conspicuously missing.⁷¹ Indeed, an examination of the temperature dependence of the magnetoresistance revealed that the local minimum at $\nu = 3 + 2/3$ does not follow the usual decreasing trend with a decreasing temperature. Therefore the opening of an energy gap, a defining property of FQHSs, could not be established at $\nu = 3 + 2/3$. Furthermore, the Hall resistance at $\nu = 3 + 2/3$ was not quantized, in fact its value was not close to the expected value of $h/(3 + 2/3)e^2$ for a FQHS. Taken together, the existence of a fractional quantum Hall ground state at $\nu = 3 + 2/3$ so far could not be established.⁷¹

In order to gain insight into FQHSs at partial filling $1/3$, one may plot the energy gaps of these FQHSs against the Coulomb energy E_c . As shown in Fig.7, the energy gaps of the FQHSs at $\nu = 2 + 1/3$, $2 + 2/3$, and $3 + 1/3$ plotted this way follow a linear trend. This suggests that these three FQHSs are similar in nature and, in the sample studied, are not close to a possible spin transition.¹¹⁵

The relationship between gaps and the Coulomb energy shown in Fig.7 may be relevant to the absence of FQHSs in the third Landau level. As shown in Fig.7, the energy gaps at the Coulomb energies calculated at $\nu = 3 + 2/3$, $4 + 1/3$, and $4 + 2/3$ extrapolate to a negative values. Within the phenomenological model embodied in Eq.(1), a disorder broadening exceeding the intrinsic gap results in a negative measured gap. Under such circumstances the formation of a FQHS is forbidden.

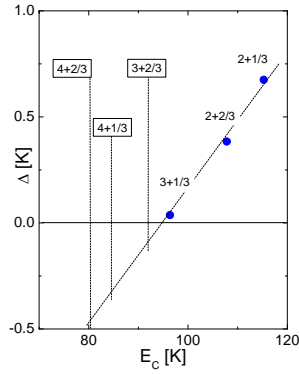


Fig. 7. Energy gaps in the second Landau level at partial filling $1/3$ versus the Coulomb energy. Data taken from Refs.70,71.

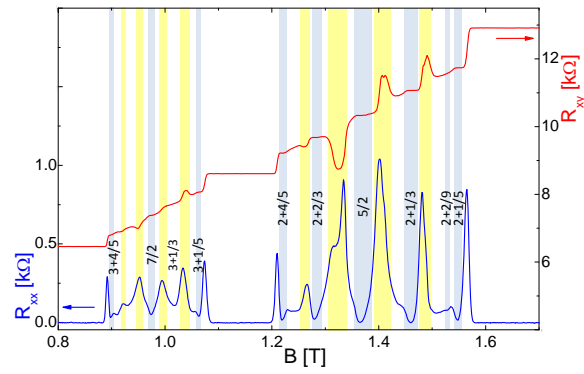


Fig. 8. Magnetotransport in the second Landau level in a sample of low density. Blue shades mark FQHSs at the labeled filling factors, whereas yellow shades show precursors of eight RIQHSs. The lower spin branch data between $B = 1.1$ and 1.7 T is adapted from Ref.176.

Based on such an argument, in the sample under investigation disorder effects are too strong for the observation of the opening of an energy gap at $\nu = 3 + 2/3$, $4 + 1/3$, and $4 + 2/3$. According to the Hartree-Fock theory,^{37,38} exact diagonalization,¹¹⁶ and density matrix renormalization group calculations,¹¹⁷ the formation of the RIQHSs in the third Landau level is usually attributed to their favorable cohesion energy as compared to that of FQHSs at partial filling $1/3$. However, it is also possible that FQHS of the third Landau level are suppressed solely because of the presence of disorder.

The most surprising feature of magnetotransport in the upper spin branch is the relative robustness of the FQHS at $\nu = 3 + 1/5$ when compared to that of the FQHS at $\nu = 3 + 1/3$.⁷¹ This result is consistent with earlier work in which a FQHS was seen at $\nu = 3 + 1/5$, but not at $\nu = 3 + 1/3$.⁴⁵ The energy gaps were found to obey the $\Delta_{3+1/3} < \Delta_{3+1/5}$ relation.⁷¹ This relationship is very unusual since an opposite inequality $\Delta_{2+1/3} > \Delta_{2+1/5}$ holds in the lower spin branch of the second Landau level^{44,70,98,118,119} and $\Delta_{1/3} > \Delta_{1/5}$ in the lowest Landau level.^{42,120} The latter two relationships are often ascribed to the robustness of flux-two composite fermions when compared to the higher order flux-four objects.¹¹ To summarize, the expected relationship between the energy gaps of the FQHSs at partial filling factors $1/3$ and $1/5$ is reversed in the upper spin branch of the second Landau level.⁷¹ This anomalous gap reversal indicates an unanticipated difference between the prominent odd denominator FQHSs forming in the second Landau level.⁷¹

Since the upper spin branch forms at higher values of the Landau level mixing parameter than the lower spin branch, the mixing effect is likely of importance. However, details of the influence of Landau level mixing are not understood. To illustrate this, magnetoresistance is shown in Fig.8 for a sample of a low electron density $n = 8.3 \times 10^{10} \text{ cm}^{-2}$. There are prominent minima developed in the mag-

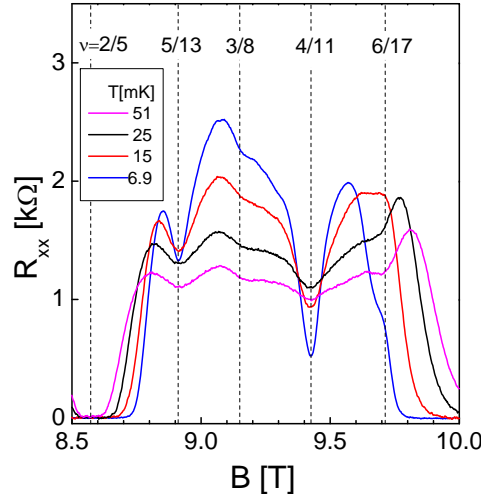


Fig. 9. Magnetotransport in the range of filling factors $1/3 < \nu < 2/5$ of the lowest Landau level. Developing FQHSs are seen at $\nu = 4/11$ and $5/13$. Adapted from Ref.128.

netoresistance and a strong Hall quantization at $\nu = 3 + 1/5$ and $3 + 4/5$, but only a weak minimum and a lack of Hall quantization at $\nu = 3 + 1/3$. These results suggest that FQHSs at partial fillings $1/5$ stay strong in the upper spin branch of the second Landau level even at significantly large values of the Landau level mixing parameter.

The above described anomalous energy gaps of the prominent odd denominator FQHSs in the upper spin branch of the second Landau level highlight the lack of understanding of these FQHSs and even elicit the provocative possibility that some of these FQHSs may be of exotic origin.⁷¹

3.3. $\nu = 4/11$ and $5/13$ fractional quantum Hall states

One of the regions of interest for the observation of novel FQHSs in the lowest Landau level is that between $1/3 < \nu < 2/5$. The observation of a local minimum in the magnetoresistance in this range at $\nu = 4/11$ and of less pronounced features at filling factors such as $\nu = 5/13$, $6/17$, and $3/8$ was an early indicator of possible fractional quantum Hall ground states.¹²¹ Initially the FQHS at $\nu = 4/11$ was interpreted as a fractional quantum Hall effect of composite fermions.¹²¹ However, theoretical work suggested that, owing to the residual interactions between the composite fermions, at $\nu = 4/11$ the ground state is a FQHS with an unusual topological order.^{122–124} This idea received strong support from a composite fermion diagonalization study over an extended Hilbert space.¹²⁵

While the theory results favoring a FQHS with a novel topological order at $\nu = 4/11$ are compelling,^{123–125} the lack of observation of an energy gap in the excitation spectrum, i.e. of incompressibility, at this and other nearby filling factors

raised the question whether fractional quantum Hall ground states can be experimentally realized. A necessary condition for the opening of a gap is a longitudinal magnetoresistance R_{xx} that decreases with temperature.

The most recent experimental work in the $1/3 < \nu < 2/5$ range focused on searching for an activated behavior. There are two reports that confirmed the development of Hall quantization and the opening of an energy gap at $\nu = 4/11$, of magnitudes 7 mK¹²⁷ and 15 mK,¹²⁸ respectively. Magnetotransport data in the $1/3 < \nu < 2/5$ range from Ref.128 are shown in Fig.9. Temperature dependence of magnetotransport at $\nu = 5/13$ was also found to be consistent with the development of an incipient gap.¹²⁸ These measurements established fractional quantum Hall ground states at $\nu = 4/11$ and $5/13$ and opened up the possibility for novel topological order in the $1/3 < \nu < 2/5$ region.

Despite considerable progress at $\nu = 4/11$ and $5/13$, transport data at other filling factors of interest, such as $\nu = 3/8$ and $6/17$, did not conclusively establish the opening of an energy gap.^{127,128} Magnetoresistance at $\nu = 3/8$ in both experiments was found to increase with a lowering temperature, precluding therefore activation. Furthermore, the filling factor $\nu = 6/17$ is extremely close to the quantized plateau associated with the $\nu = 1/3$ FQHS. A recent numerical study of the FQHS at $\nu = 6/17$ found it is described by the model of non-interacting composite fermions.¹²⁶ For now, the behavior of the magnetoresistance at $\nu = 3/8$ and $6/17$ cannot be conclusively associated with the opening of an energy gap despite the existence of a depression in R_{xx} at these filling factors.

4. Even denominator fractional quantum Hall states

The FQHS at $\nu = 5/2$ is the most notable FQHS beyond the model of non-interacting composite fermions. This FQHS was discovered⁴² and its full quantization was reported in Refs.43,44. Related FQHSs develop at other filling factors of even denominator in the GaAs/AlGaAs system at $\nu = 7/2$ ⁴⁵ and $\nu = 2 + 3/8$.⁴⁶ Even denominator FQHSs have also been seen in ZnO/MgZnO¹²⁹ and in bilayer^{114,130–132} and, most recently, in monolayer^{133,134} graphene. However, it is not yet established whether or not these latter FQHSs and the $\nu = 5/2$ FQHS in GaAs/AlGaAs share the same origin.

The instability of the Fermi sea of composite fermions and the existence of an energy gap at this filling factor is naturally explained by a Cooper-like pairing of the composite fermions.^{6,135–140} Because of constraints on the spin degree of freedom, such a pairing must necessarily be p -wave pairing.¹³⁶ The Pfaffian is the earliest description of the FQHS at $\nu = 5/2$ which is consistent with such a pairing.⁶ The Pfaffian is of considerable interest since at least some of its quasiparticles are predicted to obey exotic non-Abelian braiding statistics. However, at this filling factor there are also other topologically distinct candidates. such as the anti-Pfaffian,^{141,142} the (3,3,1) Abelian state,¹⁴³ a variational wave function based on an anti-symmetrized bilayer state,¹⁴⁴ the particle-hole symmetric Pfaffian,^{145,146} a stripe-like alternation

of the Pfaffian and anti-Pfaffian,¹⁴⁷ and other exotic states.^{148,149}

An intense effort is focused on unraveling the properties of the even denominator FQHSs. Some aspects of this effort were reviewed in Refs.^{150,151} Edge-to-edge tunneling,^{104,152–154} quasiparticle interferometry,¹⁵⁵ upstream neutral modes,¹⁰³ edge heat conduction measurements¹⁵⁶ probed the structure of the edge states at $\nu = 5/2$. However, results from these measurements do not yet offer a consensus on the origin of the $\nu = 5/2$ FQHS. Since the physics of the edge may be considerably more complicated than that of the bulk, bulk probes such as transport and heat capacity measurements¹⁵⁷ remain important in the study of the FQHS at $\nu = 5/2$. In this section we discuss results on the $\nu = 5/2$ FQHS that were learnt from recent transport data. Several experiments suggest that away from the optimal density phase transitions are allowed in the FQHS at $\nu = 5/2$. We will also discuss the energy gap and the disorder broadening of the FQHS at this filling factor in the highest quality samples. The last subsection contains results of a systematic study of the behavior of the $\nu = 5/2$ FQHS in the presence of short-range alloy disorder.

4.1. $\nu = 5/2$ fractional quantum Hall state at low electron densities

The regime of low densities for the $\nu = 5/2$ FQHS emerged as an area of interest because of the possibility of phase transitions occurring here. In the following we discuss a spin transition¹⁵⁸ and a topological phase transition at $\nu = 5/2$.¹⁵⁹ In addition, a transition from the $\nu = 5/2$ FQHS towards the quantum Hall nematic will be discussed in Sec. 6.^{160–162}

A possible phase transition in the $\nu = 5/2$ FQHS is a spin transition, from a fully spin polarized to a partially polarized state. According to experimental work performed at large magnetic fields and hence large densities, the $\nu = 5/2$ FQHS is fully spin polarized.^{163,164} However, these experiments do not rule out a partially spin polarized FQHS at low electron densities. Recent experimental work on a series of samples, including samples of density as low as $n = 4.1 \times 10^{10} \text{ cm}^{-2}$, found a region of densities at which the energy gap nearly closes.¹⁵⁸ These results have been interpreted as being consistent with a spin transition in the $\nu = 5/2$ FQHS.¹⁵⁸ While these results¹⁵⁸ are suggestive of a phase transition, a spin transition is only one of the possibilities. Indeed, while changing the density other parameters of the system may also change. Examples of such parameters are the Landau level mixing parameter, defined as the ratio of Coulomb and cyclotron energies, and the width of the quantum well. Therefore orbitally driven phase transitions may also occur when the density is changed.

As discussed earlier, theory finds that for the $\nu = 5/2$ FQHS several topologically different candidate states are allowed.^{6,141–149} If more than one of these states can be stabilized, intriguing topological phase transitions may occur at $\nu = 5/2$ between pairs of such distinct FQHSs. Such phase transitions may be driven by a parameter of the 2DEG, such as the Landau level mixing parameter κ . As an example, it was argued that a direct topological phase transition between the Pfaffian

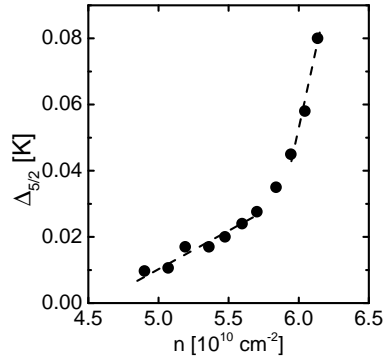


Fig. 10. Energy gap of the $\nu = 5/2$ FQHS versus density in a high quality low density sample. The anomalous trend of the energy gap at $\nu = 5/2$ versus density may be interpreted as being due to a topological phase transition. Adapted from Ref.159.

and the anti-Pfaffian may occur.^{141,142} According to numerical work, the Pfaffian and anti-Pfaffian ground states may compete as the Landau level mixing is tuned.^{87,165–173} However, due to difficulties stemming from the non-perturbative nature of the calculations and due to limited computational resources, details of a possible transition between the Pfaffian and the anti-Pfaffian at large Landau level mixing could not be firmly established.¹⁷² Nonetheless, the regime of low densities or large Landau level mixing has emerged as a region of interest for a possible topological phase transition in the $\nu = 5/2$ FQHS.

In a recent experiment on a density-tuned 2DEG,¹⁵⁹ an anomalously sharp change in the density dependence of the energy gap of the $\nu = 5/2$ FQHS was reported in the vicinity of $\kappa = 2.6$ or $n = 5.8 \times 10^{10} \text{ cm}^{-2}$. This behavior is shown in Fig.10. The origins of the observed anomalous dependence of the energy gap are not known; one possibility is a topological phase transition in the $\nu = 5/2$ FQHS.¹⁵⁹ We note that the energy gap at the apparent transition point in this experiment did not close. While the closure of the gap is generally believed to be a necessary condition for a topological phase transition, one may also envision topological transitions in which the gap does not fully close, for example in a first order phase transition. A topological phase transition in the $\nu = 5/2$ FQHS may also be induced in confined geometries by changing the confinement potential.^{154,174}

Another interesting possibility for a phase transition at $\nu = 5/2$ from a FQHS towards the quantum Hall nematic was recently revealed by measurements at high hydrostatic pressures.^{160,161} Further details of this phase transition can be found in Sec. 6.

4.2. Energy gap at $\nu = 5/2$ in pristine samples

Unraveling the effects of the disorder is an important endeavor in contemporary condensed matter physics. Disorder is well understood in the single particle regime

for example in connection with Anderson localization and the universal plateau-to-plateau transition in the integer quantum Hall effect.^{49,175} In contrast, understanding disorder in correlated electron systems, such as the 2DEG in the fractional quantum Hall regime, continues to pose serious challenges.

In the following, we will refer to samples of the highest possible mobility and, therefore, the least amount of disorder as pristine samples. The highest mobility under given growth conditions is a function of the electron density.¹³

Efforts in understanding the energy gap of the $\nu = 5/2$ FQHS examined its relationship to electron mobility μ and quantum lifetime τ_q . In the most general case, the energy gap at $\nu = 5/2$ in pristine samples did not correlate with the mobility.^{29,93,118,119,176–179} Similarly, the energy gap at $\nu = 5/2$ did not scale with the quantum lifetime.^{73,176} In fact in gated samples it was found that the quantum lifetime is approximately constant over the density range at which the energy gap at $\nu = 5/2$ decreased from its largest value to zero.^{73,119} These results are perhaps not surprising since, in contrast to the energy gap at $\nu = 5/2$, both the mobility and the quantum lifetime are parameters measured near zero magnetic field, in a regime that may be understood within a single electron description.

The phenomenological model described earlier in Sec. 3.1 offers a framework for analyzing the gap of the $\nu = 5/2$ FQHS. The use of this model for gaps measured in the second Landau level, however, poses challenges as these gaps were suspected to be smaller than the disorder broadening. In contrast, Γ at $\nu = 1/3$ is negligible as compared to Δ^{int} and the intrinsic gap may be estimated from the measured value of the gap, $\Delta^{int} \simeq \Delta$ in samples of high density.^{99,100} Therefore in order to estimate Δ^{int} at $\nu = 5/2$, one needs to measure independently two quantities: both Δ and Γ . Hence a quantitative knowledge of the disorder broadening plays a significant role in understanding the energy gaps of the exotic FQHSs. However, Γ is not directly accessible from gap measurements at $\nu = 5/2$.

To resolve this impasse, Morf and d'Ambrumenil¹⁸⁰ proposed an analysis based on the measurement of two independent quantities: the energy gaps of FQHSs at both $\nu = 5/2$ and $\nu = 7/2$ in a sample of given electron density. In addition, it was assumed that these two FQHSs have the same dimensionless intrinsic gap $\delta^{int} = \Delta^{int}/E_c$, where E_c is the Coulomb energy. The dimensionless intrinsic gap δ^{int} and disorder broadening Γ may be obtained by plotting the measured gaps at $\nu = 5/2$ and $7/2$ against the Coulomb energy and by extracting the slope and the intercept with the vertical scale of the line passing through the two points. Following this recipe,¹⁸⁰ an analysis of the gaps in a sample of electron density $n = 3.0 \times 10^{11} \text{ cm}^{-2}$ from Ref.45 yielded values $\delta^{int} = 0.014$ and $\Gamma = 1.24 \text{ K}$. A similar fit, shown in Fig.11a, on the sample from Ref.70 yielded $\delta^{int} = 0.019$ and $\Gamma = 1.5 \text{ K}$.¹⁷⁶

The analysis of the gaps proposed by Morf and d'Ambrumenil¹⁸⁰ was later extended for samples of low densities,¹⁷⁶ down to $n = 8.3 \times 10^{10} \text{ cm}^{-2}$. The intrinsic gaps as plotted against the density, shown in Fig.11b, were in reasonable agreement

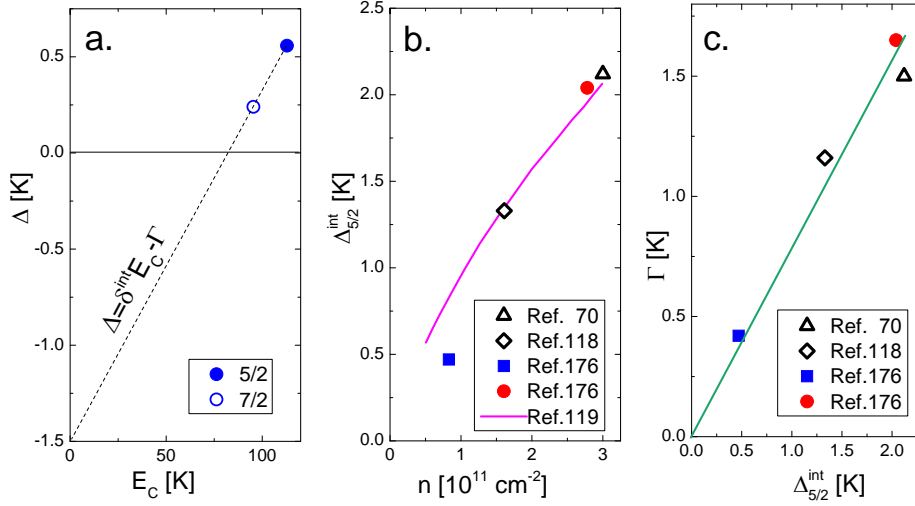


Fig. 11. Panel a: A fit to the measured gaps at even denominators used to extract the dimensionless intrinsic gap δ^{int} and the disorder broadening Γ . Data is from Ref.176. Panel b: A comparison of intrinsic gaps at $\nu = 5/2$ obtained from measurements (data points) and numerics (line). Data taken from Ref.176. Panel c: The dependence of Γ on $\Delta_{5/2}^{int}$.

with a numerical simulation that accounted for Landau level mixing within the random phase approximation.¹¹⁹ However, such an agreement can only be considered crude at best since the assumption of equal δ^{int} for the $\nu = 5/2$ and $\nu = 7/2$ FQHSs is only approximate in measurements due to the slightly different Landau level mixing parameters at these filling factors.

It is instructive to plot the calculated δ^{int} against the Landau level mixing parameter κ . The decreasing trend obtained is shown in Fig.12. It was found that a linear fit to the data extrapolates to $\delta^{int} = 0.032$ in the limit of $\kappa = 0$. This extrapolated value is in good agreement with the numerically obtained values at zero Landau level mixing: 0.02 – 0.04 from an exact diagonalization on finite size systems,¹⁸¹ 0.030 from a DMRG calculation¹⁸² and 0.031 from an exact diagonalization study adjusted for the finite width of the quantum well.¹¹⁹ The latter two figures are from extrapolations to the thermodynamic limit. Since simulations with no Landau level mixing are significantly easier than the ones that include it,¹⁷² the agreement of δ^{int} from these simulations and δ^{int} extrapolated to $\kappa = 0$ is an important confidence test of the analysis above.

Another extrapolation of interest is to large κ . The functional form for this extrapolation is not known; in Ref.176 a linear extrapolation was used. The extrapolated intrinsic gap at $\nu = 5/2$ was found to close near $\kappa \simeq 3$.¹⁷⁶ This result is consistent with the totality of observations of electron gases at low densities in the GaAs/AlGaAs system.^{158,176} This result is also consistent with observations in p -type carriers, i.e. two dimensional hole gases in GaAs/AlGaAs in which values of

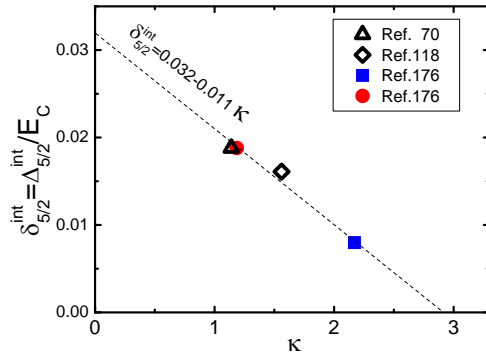


Fig. 12. Dimensionless intrinsic gaps at $\nu = 5/2$ as function of the Landau level mixing parameter κ . Dotted line is a fit through the data. Adapted from Ref.176.

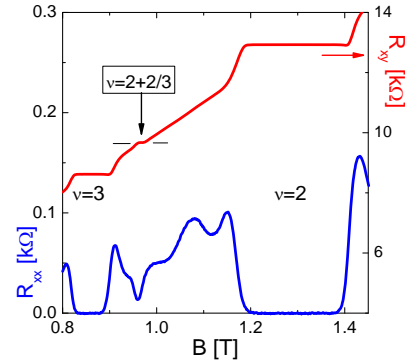


Fig. 13. Magnetotransport in the $2 < \nu < 3$ range of a p -type sample. A FQHS is seen at $\nu = 2 + 2/3$. Adapted from Ref.183.

κ are significantly larger than 3 and in which an even denominator FQHS was not observed. As an example, in Fig.13 we show the $2 < \nu < 3$ range for a hole gas with $\kappa = 14$, in which an odd denominator FQHS develops, but an even denominator FQHS is not present.¹⁸³ We note that it is widely appreciated that, besides Landau level mixing, energy gaps also depend on the width of the quantum well in its dimensionless form w/l_B . For the samples on which Fig.12 is based on, these dimensionless widths were fortuitously nearly constant.¹⁷⁶

Progress in MBE technology has resulted in a dramatic improvement of the quality of 2DEG confined not only to GaAs/AlGaAs,¹³ but also to ZnO/MgZnO structures.¹⁹ In such 2DEGs of increased mobility there is a recent report¹²⁹ of even denominator FQHSs. Measured parameters of the 2DEG in this experiment show that these even denominator FQHSs occur near $\kappa \simeq 15$.¹²⁹ According to the extrapolation to large κ shown in Fig.12, at such large values of κ a FQHS at $\nu = 5/2$ cannot be stabilized in GaAs/AlGaAs samples. This result thus raises the interesting possibility that the even denominator FQHSs in GaAs/AlGaAs and in ZnO/MnZnO may have a different origin.

Finally, it is interesting to note that, as seen in Fig.11c, the disorder broadening Γ in these samples,¹⁷⁶ extracted by the technique of Morf and d'Ambrumenil, is found to be linear with the intrinsic gap Δ^{int} . The slope of a linear fit to data in Fig.11c passing through the origin is 0.78.

4.3. Energy gap at $\nu = 5/2$ in samples with alloy disorder

Progress in MBE growth of GaAs/AlGaAs structures has produced sufficiently high quality 2DEGs to observe quantum Hall phenomena even when there was disorder intentionally added to the 2DEG. Adding disorder during the MBE growth process allowed for a high degree of its control. So far only alloy disorder was systematically

studied.^{184,185} The particular type of alloy disorder investigated consisted of minute amounts of neutral Al atoms added to the GaAs region supporting the 2DEG. Experiments on such alloy samples had a strong impact on the understanding of the plateau-to-plateau transition in the integer quantum Hall regime,^{49,175} mapping the electronic wavefunction along a direction perpendicular to the plane of the 2DEG,¹⁸⁶ and contributed to understanding of pinning of Wigner crystals.¹⁸⁷

Another successful experiment was performed on alloy samples that enabled the study of the FQHS at $\nu = 5/2$ in the presence of alloy disorder.^{185,188} These samples were based on modern sample structures assuring the high density, near $n \simeq 3 \times 10^{11} \text{ cm}^{-2}$, and high quality necessary for robust second Landau level fractional quantum Hall states. Specifically, samples were modulation-doped $\text{Al}_{0.24}\text{Ga}_{0.76}\text{As}/\text{Al}_x\text{Ga}_{1-x}\text{As}/\text{Al}_{0.24}\text{Ga}_{0.76}\text{As}$ quantum wells, where the molar Al fraction x in the quantum well was significantly less than that in the barriers.¹⁸⁵ The dependence of the scattering rate on the amount of Al introduced to the quantum well can be seen in Fig.14. The linear dependence and slope of the scattering rate on the amount of Al characterizes the alloy potential and was found to be consistent with earlier results.¹⁸⁴ Moreover, because of the small scattering rate in the pristine sample with no added impurities to the quantum well, alloy scattering exceeded the residual scattering rate in all these samples, with the exception of the one with the lowest non-zero x .¹⁸⁵

As shown in Fig.15, an increasing amount of alloy disorder decreases the mobility and it also suppresses the energy gap of the $\nu = 5/2$ FQHS.¹⁸⁸ A similar behavior was found in numerical work on the $\nu = 1/3$ FQHS, in which the strength of a Gaussian correlated white noise was increased.^{189–193} A peculiarly interesting feature of the data is revealed when the alloy samples are compared to high quality pristine, i.e. alloy-free samples. Because the mobility is not independent of the

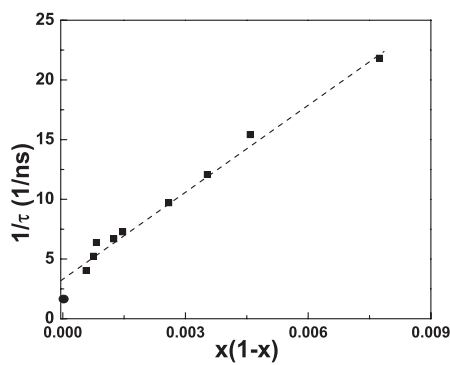


Fig. 14. The dependence of the scattering rate $1/\tau$ on alloy disorder in a series of 30 nm quantum well based alloy samples. Here x is the Al molar concentration. Adapted from Ref.185.

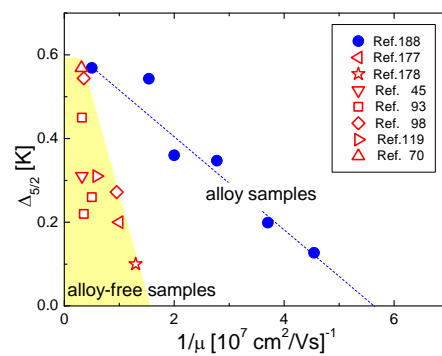


Fig. 15. The dependence of the energy gap of the $\nu = 5/2$ FQHS on inverse mobility in a set of pristine and a series of alloy samples near the density $3 \times 10^{11} \text{ cm}^{-2}$. Adapted from Ref.188.

sample density, in Fig.15 only pristine samples from the literature are shown that have their density in the $2.65 \times 10^{11} \leq n \leq 3.2 \times 10^{11} \text{ cm}^{-2}$ range, i.e. close to that of the alloy samples. Energy gaps for the pristine samples are clustered in the area shaded in yellow in Fig.15, but shown no correlation with $1/\mu$. In contrast, the energy gap in the series of alloy samples shows a linear functional dependence on the inverse mobility $1/\mu$. This suggests that when in a series of similar samples one particular type of disorder dominates, such as in the series of alloy samples, the energy gap and the mobility appear to be correlated.¹⁸⁸ However, in samples which have different types of dominating disorder, a correlation between the energy gap and the mobility is not expected.¹⁸⁸

An interesting feature of the data shown in Fig.15 is that a strong $\nu = 5/2$ FQHS with $\Delta_{5/2} = 127 \text{ mK}$ develops in the alloy sample with $\mu = 2.2 \times 10^6 \text{ cm}^2/\text{Vs}$. This is surprising, since at such a low mobility a $\nu = 5/2$ FQHS has never been observed in pristine, alloy-free samples. Indeed, for pristine, alloy-free samples with density near $n = 3 \times 10^{11} \text{ cm}^{-2}$, the threshold mobility value for the observation of a $\nu = 5/2$ FQHS is $\mu_c \simeq 7 \times 10^6 \text{ cm}^2/\text{Vs}$. The mobility threshold for a fully quantized $\nu = 5/2$ FQHS is therefore significantly lowered in the presence of alloy disorder and, therefore, the $\nu = 5/2$ FQHS is robust to the presence of alloy disorder.¹⁸⁸ Alloy disorder does not appear to be as detrimental to the development of the $\nu = 5/2$ FQHS as the residual disorder unintentionally added during sample growth.¹⁸⁸ The gap $\Delta_{5/2}$ in the series of alloy samples studied closes at an extrapolated threshold of $\mu_c^{\text{alloy}} \simeq 1.8 \times 10^6 \text{ cm}^2/\text{Vs}$.

Al is a neutral impurity and it perturbs the GaAs crystal on a subnanometer length scale. Alloy disorder is thus a type of disorder that generates a short-range scattering potential. Other types of disorder, due to either short- or long-range scattering potentials, have not yet been systematically studied.

5. Studies of reentrant integer quantum Hall states

RIQHSs are collectively localized ground states associated with electronic bubble phases.^{37–41} They were discovered in the third and higher Landau levels^{40,41} and later also seen in the second Landau level.⁴⁵ There are also two reports of RIQHSs in the lowest Landau level, however the nature of these RIQHSs may be different from those forming in higher Landau levels.^{194,195} In this section we discuss recent results on RIQHSs in the second Landau level. Topics include the magnetoresistive fingerprints of the RIQHSs in high mobility samples, a discussion of the precursors of the RIQHSs, and a summary of new RIQHSs.

Transport signatures of RIQHSs are $R_{xx} = 0$ and $R_{xy} = h/ie^2$, where $i = \text{integer}$.^{40,41} However, in contrast to integer quantum Hall states, RIQHSs are centered at a filling factor other than an integer. A characteristic of the RIQHSs is that they are separated from the nearby integer quantum Hall plateaus by distinct resistive signatures.^{40,41} Regions shaded in yellow in Fig.4 and Fig.16 mark several RIQHSs forming in the second Landau level. The above transport signatures of RIQHSs

indicate a pinned insulator and the reentrant property was argued to distinguish RIQHSs from an Anderson insulator.^{45,196}

Following the discovery of RIQHSs, efforts on these states were focused on establishing their fundamental signatures in magnetotransport, on their filling factors of formation,^{45,95,97,197} on gaining an understanding of their energy scale,^{95,197} on their microwave pinning modes,^{198–200} on thermopower,²⁰¹ on their electrical breakdown,^{196,202–206} and most recently, on their attenuation of surface acoustic waves.^{207,208}

RIQHSs develop at temperatures higher than 100 mK in the third Landau level and at tens of mK in the second Landau level. Therefore the use of a He-3 immersion cell to generate ultra-low temperatures may seem unnecessary in their study. Nonetheless, immersion cells have contributed to the RIQHSs in an unexpected way: the large heat capacity of the He-3 liquid provided enhanced temperature stability. Since the magnetoresistance of RIQHS near their onset changes extremely rapidly with temperature, the high temperature stability afforded by the immersion cell setup allowed for a careful mapping of these temperature sensitive features.^{95,97,197}

5.1. Resistive fingerprints of reentrant integer quantum Hall states

The vanishing longitudinal magnetoresistance and Hall quantization to an integer value were transport features of RIQHSs clearly identified at their discovery.^{40,41,45} It later became apparent that samples with improved quality exhibit additional transport features associated with RIQHSs. One such feature is the flanking of the longitudinal magnetoresistance by sharp peaks at both ends of the magnetic field. In other words, the region of vanishing magnetoresistance of a RIQHS is delimited by two sharp peaks. As seen in Fig.4, these two sharp resistance peaks in the flanks of RIQHSs are present in both spin branches of the second Landau level.⁹⁵ Similar sharp peaks are also delimiting the RIQHSs in the third Landau level (not shown).¹⁹⁷

As the temperature is raised, the two sharp peaks in R_{xx} in the flanks of RIQHSs persist.⁹⁵ However, the two sharp peaks in R_{xx} move closer to each other and, as a result, the width of the vanishing R_{xx} plateau shrinks. Such a trend may be seen in Fig.16 for several RIQHSs and may be examined in detail in the middle row of panels of Fig.18 for one of the RIQHSs labeled $R2b$. At the temperature of $T = 32.6$ mK the magnetoresistance shown in Fig.18b no longer vanishes, but it consists of two peaks with a non-zero local minimum in between them. The location in filling factor of this minimum is T -independent to a good degree and defines the central filling factor ν_c of the RIQHS. At $T = 35.7$ mK the two spikes of $R_{xx}(\nu)$ have moved closer to each other; between them there is still a local minimum, albeit with a large resistance.

A second transport feature associated with the RIQHSs becomes apparent by measuring the temperature dependence $R_{xx}(T)|_{\nu}$ at a fixed ν or B -field.⁹⁵ One may visualize such a $R_{xx}(T)|_{\nu}$ curve as a cut in the $R_{xx}(\nu, T)$ manifold at a given

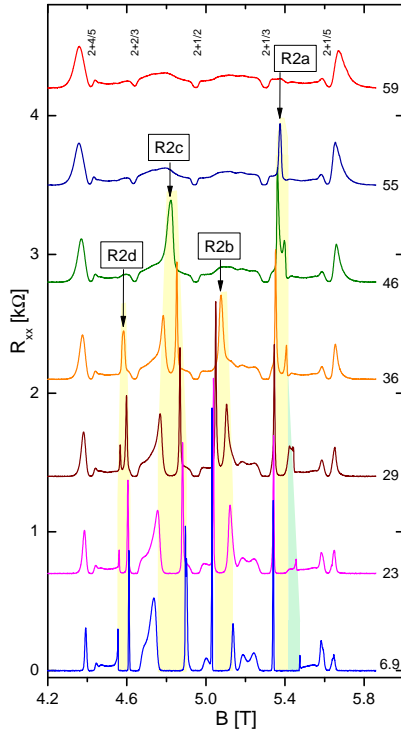


Fig. 16. Waterfall plot of magnetoresistance in the lower spin branch of the second Landau level, as measured at different temperatures. Traces are labeled by temperatures in mK. Adapted from Ref.97.

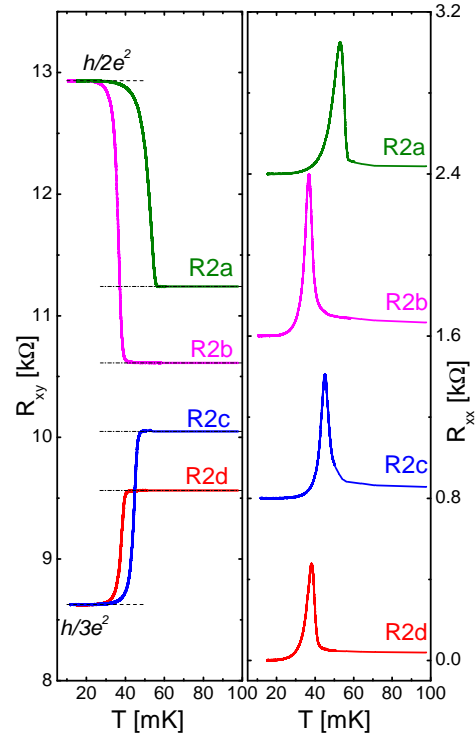


Fig. 17. Temperature dependence of R_{xx} and R_{xy} measured at the central filling factor of the RIQHSs labeled $R2a$, $R2b$, $R2c$, and $R2d$. Sharp peaks in R_{xx} mark the onset temperatures of the RIQHSs. Adapted from Ref.95.

filling factor of choice ν . Such $R_{xx}(T)|_{\nu}$ and $R_{xy}(T)|_{\nu}$ curves measured at $\nu = \nu_c$ are shown in Fig.17 for the RIQHSs of the lower spin branch of the second Landau level. It was found that, as the temperature is lowered, the Hall resistance $R_{xy}(T)|_{\nu=\nu_c}$ changes from its classical value to its quantized value, either $h/2e^2$ or $h/3e^2$. At the same time the curve $R_{xx}(T)|_{\nu=\nu_c}$ exhibits a sharp peak. The inflection point in $R_{xy}(T)|_{\nu=\nu_c}$ and the sharp peak in $R_{xx}(T)|_{\nu=\nu_c}$ coincide and may be interpreted as the onset temperature of the RIQHS. An analysis of the onset temperatures of the RIQHSs in the second Landau level obtained this way found that they scale with the Coulomb energy, demonstrating the collective nature of these RIQHSs.⁹⁵ Fig.18 may be used to correlate data collected at constant $\nu = \nu_c$ with data at constant temperature for both R_{xx} and R_{xy} .

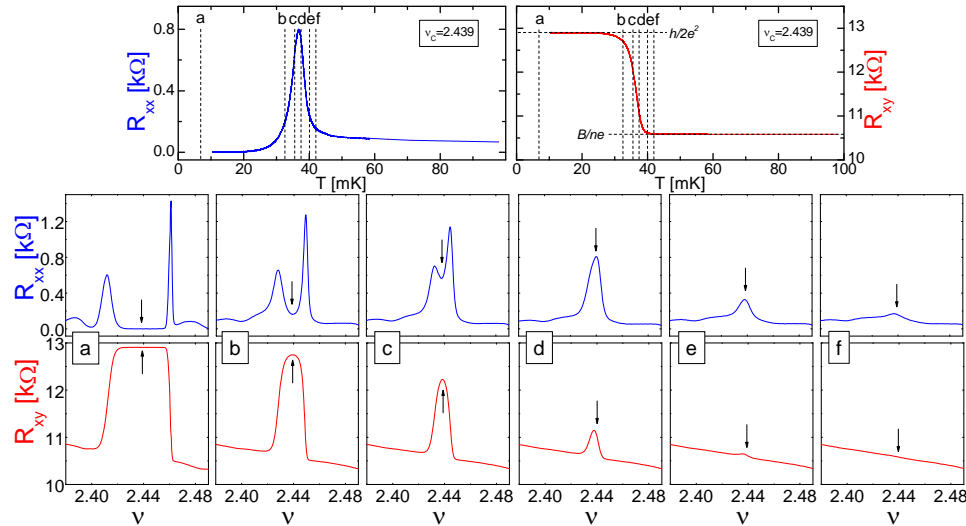


Fig. 18. Correlation of cuts along different axes in the $R_{xx}(\nu, T)$ and $R_{xy}(\nu, T)$ manifolds in the region of the RIQHS labeled as $R2b$. The two top panels show the temperature dependence at $\nu = \nu_c$, whereas the two lower rows of panels show ν dependence at fixed temperatures. Data in panels a , b , c , d , e , and f are collected at the temperatures $T = 6.9, 32.6, 35.7, 37.7, 40.0$, and 41.7 mK. Arrows mark the central filling factor $\nu = \nu_c$. Precursor of the RIQHS are seen in panels d , e , and f . Data taken from Ref.95.

5.2. The precursor of reentrant integer quantum Hall states

When comparing the $T = 35.7$ and 37.7 mK traces shown in Fig.18c and Fig.18d, respectively, one notices that a modest increase in T of only 2 mK results in a qualitative change in the magnetoresistance of a RIQHS from a double peak structure to a single peak in $R_{xx}(\nu)$. As the temperature is further raised, this single peak rapidly decreases until it merges into a low resistance background. Since the single peaks in R_{xx} marked by arrows in Fig.18d, Fig.18e, and Fig.18f may also be associated with RIQHSs, even though the magnetoresistance does not vanish and the Hall resistance is far from quantization. These single peaks are thus signatures of RIQHSs at the highest temperatures and they may be associated with precursors of the RIQHSs. Simultaneously with the described changes in R_{xx} , R_{xy} evolves from the quantized value $h/2e^2$ at the lowest temperatures toward its classical value B/ne .

Precursors of RIQHSs, as defined above, can be seen for each RIQHS both in the second Landau level⁹⁵ (see Fig.16) and also the third Landau level.¹⁹⁷ The concept of precursor of a RIQHS also provides a natural explanation for the observation of single peaks in R_{xx} in several experiments in the regions of the RIQHSs.^{98,118} Furthermore, eight precursors of RIQHSs also develop in the second Landau level of a sample¹⁷⁶ of very low density $n = 8.3 \times 10^{10} \text{ cm}^{-2}$; these precursors are marked by yellow shading in Fig.8.

Recently RIQHSs have also been observed in high quality graphene.²⁰⁹ These results highlight the universal, host-independent physics at play in the formation of the RIQHSs. It is interesting to note that in Ref.209 only the RIQHS labeled *R6a* is fully developed, i.e. for which $R_{xx} = 0$ and Hall resistance quantized to an integer. At other symmetry related filling factors in the regions labeled *R6b*, *R7a*, and *R7b*, a peak in R_{xx} was observed which, following the terminology discussed, is the signature of precursors of RIQHSs.

5.3. Proliferation of reentrant integer quantum Hall states in the second Landau level

At the time of the discovery of the RIQHSs in the second Landau level, eight such RIQHSs were observed.⁴⁵ These RIQHSs are some of the most fragile, as their onset temperatures do not exceed 55 mK.^{95,197} Besides these eight RIQHSs, in the second Landau level there are three other magnetoresistance features that can be associated with additional RIQHSs.

One such additional RIQHSs was discovered as a split-off phase of the RIQHS in the second Landau level developing at the largest magnetic field.⁴⁶ This split-off phase, labeled *R2 \tilde{a}* in Refs.95,97, is fully developed, since at the lowest temperatures accessed $R_{xx} = 0$ and $R_{xy} = h/2e^2$. This RIQHS is also shown in Fig.19a.

Another developing RIQHS at $2 + 1/5 < \nu < 2 + 2/9$ was identified in Ref.197 and it is labeled as *R2r* in Fig.19a. Using the terminology introduced earlier, the magnetoresistive behavior of *R2r* is consistent with that associated with a precursor

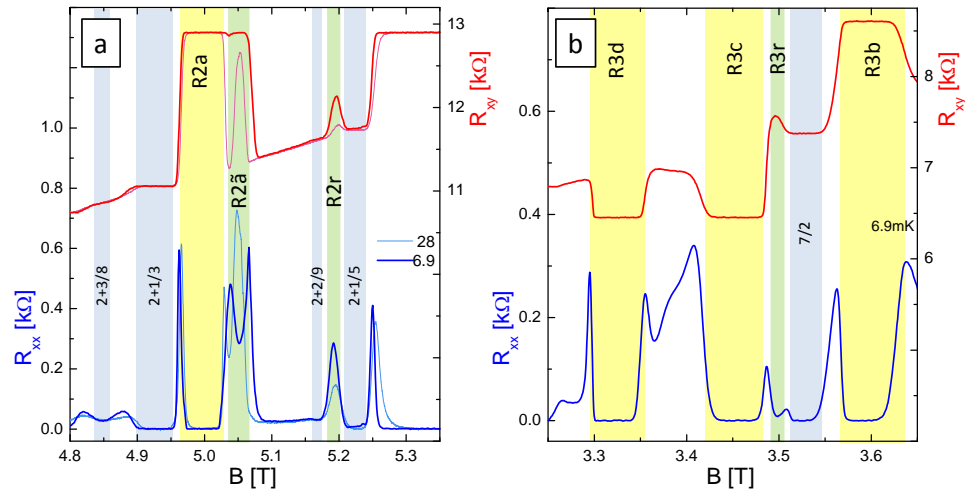


Fig. 19. Magnetotransport in the second Landau level exhibiting an increased number of RIQHSs. RIQHSs discovered in Ref.45 are shaded in yellow, any additional RIQHSs are shaded in green, and FQHSs are shaded in blue. The $T = 6.9$ mK traces in panel *a* are from Ref.197. Traces in panel *b* are from Ref.71.

of a RIQHS. Indeed, the peak in R_{xx} increases and the value of R_{xy} moves closer to $h/2e^2$ as the temperature is lowered. The nature of $R2r$ is uncertain, but it may be related to the reentrant insulating phase of the lowest Landau level that forms in the range between $1/5 < \nu < 2/9$ range and which was associated with the reentrant Wigner crystal.²¹⁰ $R2r$ could also be related to the Wigner crystal forming in the flanks of integer plateaus.

In addition, an interesting incipient RIQHS was also detected in the upper spin branch of the second Landau level, near $\nu = 7/2$.⁷¹ This incipient RIQHS is labeled with $R3r$ in Fig.19b. The magnetoresistance in this region has a distinct local minimum. An intriguing feature of this ground state is that instead of a Hall resistance moving toward $h/4e^2$, the Hall resistance appears to move towards $h/3e^2$. This latter property suggests that $R3r$ is different from other RIQHSs nearby, such as the one labeled $R3c$ in Fig.19b.

The development of an increasing number of RIQHs in the second Landau level indicates that the competition between bubble phases and other ground states in this region is more intricate than previously thought.

6. High pressure studies of the second Landau level

Hydrostatic pressure is widely used in probing condensed matter systems, such as superconductors and correlated electron systems. Pressure decreases the lattice constant of a crystal. This has profound effects on crystal properties, since the Bloch wavefunctions supported by the crystal are changed. As a consequence, both the electronic and the phononic degrees of freedom are affected. Of particular importance is the impact of high pressure on the band parameters of an electronic system. Examples of quantities tuned by pressure are the dielectric constant, effective mass, Landé g-factor, band energies, and donor energy levels.

The effect of hydrostatic pressure on 2DEGs in GaAs/AlGaAs structures is well-documented. Information of the effective mass, band energies, and pressure dependence of the electron density is found in the early literature.²¹¹ In addition, high pressure experiments manipulating the g-factor yielded significant knowledge on the spin polarization of FQHSs forming in the lowest Landau level.²¹²

More recent use of hydrostatic pressures has contributed to the physics of half-filled Landau level. This section contains a brief account of these experiments. It is well known that, depending on the number of filled Landau levels, half-filled single layer 2DEGs hosted in GaAs/AlGaAs have three distinct ground states. In the lowest Landau level, at $\nu = 1/2$ and $3/2$, there is a featureless Fermi sea of composite fermions.¹⁰¹ In other Landau levels ordered ground states develop. Indeed, in the second Landau level, at $\nu = 5/2$ and $7/2$, fractional quantum Hall states were found.^{42,45} Finally, in high Landau levels, at $\nu = 9/2, 11/2, 13/2, \dots$, the ground state is the quantum Hall nematic.^{40,41} The quantum Hall nematic³⁹ is closely related to the stripe phase predicted by the Hartree-Fock theory.^{37,38}

A peculiar feature of the ordered ground states forming at half filling is that,

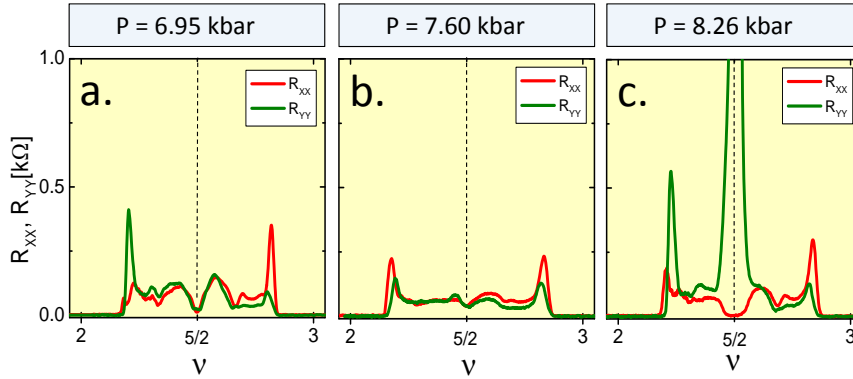


Fig. 20. Longitudinal magnetoresistance at $T \approx 12$ mK as measured in the second Landau level along two mutually perpendicular crystallographic axes of the GaAs. Green traces show R_{xx} measured along the $[1\bar{1}0]$ crystal direction, whereas red traces show R_{yy} as measured along the $[110]$ crystal direction. As the pressure is increased, at $\nu = 5/2$ the following sequence of ground states is observed: an isotropic FQHS (panel a), a nearly isotropic Fermi liquid (panel b), and the quantum Hall nematic (panel c). Adapted from Ref.160.

until recently, in clean enough samples and at low enough temperatures only one type of order seemed to develop. Thus a phase transition between the two different ordered phases, the FQHS and the quantum Hall nematic, could not be realized in purely perpendicular magnetic fields. This was surprising for two reasons. First, early theoretical work indicated that a phase transition between a FQHS and the stripe phase is allowed.²¹³ Second, experimental work has clearly indicated that the $\nu = 5/2$ FQHS is close to a nematic phase. Indeed, experiments in tilted magnetic fields have shown that the isotropic FQHS at $\nu = 5/2$ is superseded by an anisotropic nematic phase at relatively modest tilt angles.^{214,215} Nonetheless, during the three decade long history of experimental studies at $\nu = 5/2$, a nematic phase at this filling factor has never been seen in magnetic fields applied perpendicularly to the 2DEG. As a result, in a large body of numerical work focused at $\nu = 5/2$, the ground state obtained was typically compared to the Pfaffian; the quantum Hall nematic, with a few exceptions,^{169,213} was not considered a viable ground state at $\nu = 5/2$.

A first indication that in the second Landau level order other than the topological order of a FQHS may be present came from an experiment on a low density sample¹⁵⁸ in which an incipient anisotropy was reported at $\nu = 7/2$. The observed resistance anisotropy was 2. Subsequent work on 2DEG at high hydrostatic pressures revealed resistance anisotropy at both $\nu = 5/2$ ^{160,161} and $7/2$.¹⁶² Furthermore, similarly to the levels of anisotropy measured at $\nu = 9/2$, the anisotropy observed in these latter experiments^{160–162} reached extreme values exceeding 1000.

In Fig.20 we summarize salient features of the longitudinal resistance as measured at three different pressures. Since the GaAs/AlGaAs sample was mounted in a commercial pressure clamp cell, electron thermalization to the base temperature of

the refrigerator was no longer possible. The electronic temperature in these experiments was estimated to be $T \approx 12$ mK.¹⁶⁰ Fig.20a, Fig.20b, and Fig.20c show R_{xx} and R_{yy} , magnetoresistance data collected along two mutually perpendicular crystal axes of GaAs at the pressures of 6.95, 7.60, and 8.26 kbar, respectively. Data shown are consistent with the following sequence of ground states of the 2DEG at $\nu = 5/2$: a rotationally invariant FQHS at $P = 6.95$ kbar, a ground state close to an isotropic Fermi fluid at $P = 7.60$ kbar, and a quantum Hall nematic at $P = 8.26$ kbar. Because at $T \approx 12$ mK the isotropic liquid is observed in an extremely narrow range of pressures, it was argued that data from Fig.20 are suggestive of a direct quantum phase transition from the FQHS to the quantum Hall nematic in the limit of zero temperatures.¹⁶⁰ This quantum phase transition occurs in the sample studied at the critical pressure of $P_c \simeq 7.8$ kbar. Since the electron density is pressure dependent, the density at the critical pressure was $n_c = 1.1 \times 10^{11}$ cm⁻² in this experiment.¹⁶⁰ Later work mapping out the temperature dependence of the phases strengthened the argument of a direct phase transition in the limit of zero temperatures.¹⁶¹

There are several reasons to believe that the nematic seen at $\nu = 5/2$ at high pressures, shown in Fig.20c, is likely similar in nature to the quantum Hall nematic developing at $\nu = 9/2$ and other high value filling factors in samples in the ambient.¹⁶⁰ First, they are both centered at half-integer filling factors. Second, the temperature dependence of the magnetoresistance is similar in both cases: it is isotropic above the nematic onset temperature and it has a very abrupt, almost exponential onset. Third, both the nematic near both $\nu = 5/2$ and $\nu = 9/2$ develop over a relatively narrow range of filling factors. Indeed, the range of fillings for the nematic in both cases is about $\Delta\nu \simeq 0.15$. This value is in sharp contrast to the significantly larger $\Delta\nu \simeq 0.6$ range of filling factors of nematicity developing near $\nu = 5/2$ in tilted magnetic fields. This is significant, because an ordered phase induced by an external intensive parameter is not necessarily identical to a spontaneously ordered phase. For example, the magnetized phase induced in a paramagnet when placed in an external magnetic field is not identical to the spontaneous ferromagnetic phase, as the two do not share the same correlation functions. In tilted field experiments on 2DEGs the symmetry breaking field favoring nematicity is the in-plane component of the magnetic field. While the nematic phase at $\nu = 5/2$ forming in tilted magnetic fields is likely related to the nematic forming at $\nu = 5/2$ at high pressure but in the absence of any symmetry breaking fields, the exact nature of this relationship is yet to be determined.

The importance of data shown in Fig.20 is twofold. First, it was established that the quantum Hall nematic may be stabilized at $\nu = 5/2$ in the absence of an in-plane magnetic field. Second, it was pointed out that the phase transition from a FQHS to the quantum Hall nematic is of a special type.¹⁶⁰ Indeed, this phase transition involves a FQHS, which is a topological phase, and the quantum Hall nematic, which is a transitional Landau phase with a broken symmetry. Phase transitions between two Landau phases are well known. Furthermore, recent intense investigations

of phase transitions between two topologically distinct phases have significantly contributed to their understanding. However, phase transitions between the two distinct classes of phases, such as the transition from a fractional quantum Hall state to the nematic, remain rare and present an opportunity for further theoretical development.^{216–221}

One may gain further insight into the transition by investigating it in the upper spin branch of the second Landau level. Such studies confirmed a qualitatively similar phase transition at filling factor $\nu = 7/2$. It was shown that in a purely perpendicular magnetic field only even denominator FQHSs may be involved in the FQHS-to-nematic phase transition, highlighting therefore an interesting competition between paired states of composite fermions and nematicity.¹⁶² Furthermore, in this study it was also shown that the role of the pressure is to tune the electron-electron interaction; data suggest that a FQHS-to-nematic phase transition may also be induced by other means of tuning the electron-electron interaction.¹⁶²

7. Conclusions

In this chapter we addressed a few topics on the electron gas confined to GaAs/AlGaAs hosts. The study of this system presents an opportunity to learn about the effects of the Coulomb interaction on the various topological phases and their competition with charge ordered phases in a clean environment. We discussed recently discovered FQHSs, the effect of the disorder on the even denominator FQHSs, novel transport features of the RIQHSs, and recently discovered phase transitions at even denominator filling factors. Many of these results were enabled by the use of ultra-low temperature and of high pressure techniques. However, the topics covered barely scratched the surface of the ongoing research on this and related systems. As the purity of different materials improves, the effects of interactions in those materials will come to the fore. It is then expected that the interplay of interactions and topology will lead to new physics beyond that of single-electron band structure in the growing family of topological materials. Other results, such as the competition of pairing and nematicity in half-filled Landau levels, revealed a strong connection between the 2DEG and other strongly correlated materials. Research on the 2DEG in the fractional quantum Hall regime will certainly impact efforts on these materials and will continue to present future opportunities for discovery.

Acknowledgments

I would like to thank Dan Tsui for introducing me to fractional quantum Hall physics and Jian-Sheng Xia for sharing information about the He-3 immersion cell. Measurements would have not been possible without the samples of exceptional quality grown by Loren Pfeiffer and Kenneth West at Princeton and by my colleague at Purdue, Michael Manfra. I am grateful to Ashwani Kumar, Nodar

Samkharadze, Nianpei Deng, Ethan Kleinbaum, Katherine Schreiber, and Vidhi Shingla for their tireless work in the lab and for their original contributions to the topics discussed. Last but not least, I have benefited from numerous discussions with Nicholas d’Ambrumenil, Rudro Biswas, Rui-Rui Du, Eduardo Fradkin, James Eisenstein, Lloyd Engel, Jainendra Jain, Koji Muraki, Wei Pan, Zlatko Papić, Steve Simon, Jurgen Smet, and Michael Zudov. This work was supported by the NSF-DMR 1904497 and by the DOE BES award DE-SC0006671.

References

1. K. von Klitzing, G. Dorda, and M. Pepper, New Method for High-Accuracy Determination of the Fine-Structure Constant Based on Quantized Hall Resistance, *Phys. Rev. Lett.* **45**, 494–497 (1980).
2. D.C. Tsui, H.L. Stormer, and A.C. Gossard, Two-Dimensional Magnetotransport in the Extreme Quantum Limit, *Phys. Rev. Lett.* **48**, 1559–1562 (1982).
3. R.B. Laughlin, Anomalous Quantum Hall Effect: An Incompressible Quantum Fluid with Fractionally Charged Excitations, *Phys. Rev. Lett.* **50**, 1395–1398 (1983).
4. J.K. Jain, Composite-fermion Approach for the Fractional Quantum Hall Effect, *Phys. Rev. Lett.* **63**, 199–202 (1989).
5. B.I. Halperin, P.A. Lee, and N. Read, Theory of the Half-Filled Landau Level, *Phys. Rev. B* **47**, 7312–7343 (1993).
6. G. Moore and N. Read, Nonabelions in the Fractional Quantum Hall Effect, *Nucl. Phys. B* **360**, 362–396 (1991).
7. N. Read and E. Rezayi, Beyond Paired Quantum Hall States: Parafermions and Incompressible States in the First Excited Landau Level, *Phys. Rev. B* **59**, 8084–8092 (1999).
8. X.G. Wen, *Quantum Field Theory of Many-Body Systems*. (Oxford University Press, Oxford, UK, 2004).
9. T.H. Hansson, M. Hermanns, S.H. Simon, and S.F. Viefers, Quantum Hall Physics: Hierarchies and Conformal Field Theory Techniques, *Rev. Mod. Phys.* **89**, 025005 (2017).
10. H.L. Stormer, D.C. Tsui, and A.C. Gossard, The Fractional Quantum Hall Effect, *Rev. Mod. Phys.* **71**, S298–S305, (1999).
11. J.K. Jain, *Composite Fermions*. (Cambridge University Press, Cambridge, England, 2007).
12. J.K. Jain, Composite Fermion Theory of Exotic Fractional Quantum Hall Effect *Ann. Rev. Cond. Matter Phys.* **6**, 39–62 (2015).
13. L. Pfeiffer and K.W. West, The Role of MBE in Recent Quantum Hall Effect Physics Discoveries, *Physica E* **20**, 57–64 (2003).
14. T.S. Lay, J.J. Heremans, Y.W. Suen, M.B. Santos, K. Hirakawa, M. Shayegan, and A. Zrenner, High-quality Two-dimensional Electron System Confined in an AlAs Quantum Well, *Appl. Phys. Lett.* **62**, 3120–3122 (1993).
15. B. A. Piot, J. Kunc, M. Potemski, D. K. Maude, C. Betthausen, A. Vogl, D. Weiss, G. Karczewski, and T. Wojtowicz, Fractional quantum Hall effect in CdTe, *Phys. Rev. B* **82**, 081307 (2010).
16. K. Lai, W. Pan, D.C. Tsui, S. Lyon, M. Mühlberger, and F. Schäffler, Two-Flux Composite Fermion Series of the Fractional Quantum Hall States in Strained Si, *Phys. Rev. Lett.* **93**, 156805 (2004).
17. Q. Shi, M.A. Zudov, C. Morrison, and M. Myronov, Spinless Composite Fermions in an Ultrahigh-Quality Strained Ge Quantum Well, *Phys. Rev. B* **91**, 241303 (2015).

18. O.A. Mironov, N. d'Ambrumenil, A. Dobbie, D.R. Leadley, A.V. Suslov, and E. Green, Fractional Quantum Hall States in a Ge Quantum Well, *Phys. Rev. Lett.* **116**, 176802 (2016).
19. J. Falson and M. Kawasaki, A review of the quantum Hall effects in MgZnO/ZnO heterostructures, *Rep. Prog. Phys.* **81**, 056501 (2018).
20. T.M. Kott, B. Hu, S.H. Brown, and B.E. Kane, Valley-Degenerate Two-Dimensional Electrons in the Lowest Landau Level, *Phys. Rev. B* **89**, 041107 (2014).
21. Y. Monrakha and K. Kono, *Two-Dimensional Coulomb Liquids and Solids*. (Springer-Verlag, Berlin Heidelberg, 2004).
22. A.K. Geim and K.S. Novoselov, The Rise of Graphene, *Nature Materials* **6**, 183–191 (2007).
23. S. Manzeli, D. Ovchinnikov, D. Pasquier, O.V. Yazyev, and Andras Kis, 2D Transition Metal Dichalcogenides, *Mature Reviews Materials* **2**, 1–15 (2017).
24. F. Yang, Z. Zhang, N.Z. Wang, G.J. Ye, W. Lou, X. Zhou, K. Watanabe, T. Taniguchi, K. Chang, X.H. Chen, and Y. Zhang, Quantum Hall Effect in Electron-Doped Black Phosphorus Field-Effect Transistors, *Nano Lett.* **18**, 6611–6616 (2018).
25. M. Yankowitz, J. Xue, D. Cormode, J.D. Sanchez-Yamagishi, K. Watanabe, T. Taniguchi, P. Jarillo-Herrero, P. Jacquod, and B.J. LeRoy, Emergence of Superlattice Dirac Points in Graphene on Hexagonal Boron Nitride, *Nature Physics* **8**, 382–386 (2012).
26. C.R. Dean, L. Wang, P. Maher, C. Forsythe, F. Ghahari, Y. Gao, J. Katoch, M. Ishigami, P. Moon, M. Koshino, T. Taniguchi, K. Watanabe, K.L. Shepard, J. Hone, and P. Kim, Hofstadter's Butterfly and the Fractal Quantum Hall Effect in Moiré Superlattices, *Nature* **497**, 598–602 (2013).
27. Y. Cao, V. Fatemi, S. Fang, K. Watanabe, T. Taniguchi, E. Kaxiras, and P. Jarillo-Herrero, Unconventional Superconductivity in Magic-Angle Graphene Superlattices, *Nature* **556**, 43–50 (2018).
28. D.G. Schlom and L.N. Pfeiffer, Upward mobility rocks!, *Nature Materials* **9**, 881–883 (2010).
29. V. Umansky, M. Heiblum, Y. Levinson, J. Smet, J. Nübler, and M. Dolev, MBE Growth of Ultra-Low Disorder 2DEG with Mobility Exceeding $35 \times 10^6 \text{ cm}^2/\text{Vs}$, *J. Cryst. Growth* **311**, 1658–1661 (2009).
30. M.J. Manfra, Molecular Beam Epitaxy of Ultra-High-Quality AlGaAs/GaAs Heterostructures: Enabling Physics in Low-Dimensional Electronic Systems, *Annu. Rev. Condens. Matter Phys.* **5**, 347–373 (2014).
31. C. Reichl, J. Chen, S. Baer, C. Rössler., T. Ihn, K. Ensslin, W. Dietsche, and W. Wegscheider, Increasing the $\nu = 5/2$ Gap Energy: an Analysis of MBE Growth Parameters, *New Journal of Physics* **16**, 023014 (2014).
32. J.D. Watson, G.A. Csáthy, and M.J. Manfra, Impact of Heterostructure Design on Transport Properties in the Second Landau Level of In Situ Back-Gated Two-Dimensional Electron Gases, *Phys. Rev. Applied* **3**, 064004 (2015).
33. D. Kamburov, K.W. Baldwin, K.W. West, M. Shayegan, and L.N. Pfeiffer, Interplay Between Quantum Well Width and Interface Roughness for Electron Transport Mobility in GaAs Quantum Wells, *Appl. Phys. Lett.* **109**, 232105 (2016).
34. G.C. Gardner, S. Fallahi, J.D. Watson, and M.J. Manfra, Modified MBE Hardware and Techniques and Role of Gallium Purity for Attainment of Two Dimensional Electron Gas Mobility $> 35 \times 10^6 \text{ cm}^2/\text{Vs}$ in AlGaAs/GaAs Quantum Wells Grown by MBE, *J. Cryst. Growth* **441**, 71–77 (2016).
35. Y.J. Chung, K.W. Baldwin, K.W. West, M. Shayegan, and L.N. Pfeiffer, Surface Segregation and the Al Problem in GaAs Quantum Wells, *Phys. Rev. Materials* **2**,

- 034006 (2018).
36. M. Shayegan, "Case for the Magnetic-Field-Induced Two Dimensional Wigner Crystal", in *Perspectives in Quantum Hall Effects*. 343–384 (Wiley, 2004).
 37. A.A. Koulakov, M.M. Fogler, and B.I. Shklovskii, Charge Density Wave in Two-Dimensional Electron Liquid in Weak Magnetic Field, *Phys. Rev. Lett.* **76**, 499–502 (1996).
 38. R. Moessner and J.T. Chalker, Exact Results for Interacting Electrons in High Landau Levels, *Phys. Rev. B* **54**, 5006–5015 (1996).
 39. E. Fradkin and S.A. Kivelson, Liquid-Crystal Phases of Quantum Hall Systems, *Phys. Rev. B* **59**, 8065–8072 (1999).
 40. M.P. Lilly, K.B. Cooper, J.P. Eisenstein, L.N. Pfeiffer, and K.W. West, Evidence for an Anisotropic State of Two-Dimensional Electrons in High Landau Levels, *Phys. Rev. Lett.* **82**, 394–397 (1999).
 41. R.R. Du, D.C. Tsui, H.L. Stormer, L.N. Pfeiffer, K.W. Baldwin, and K.W. West, Strongly Anisotropic Transport in Higher Two-Dimensional Landau Levels, *Solid State Commun.* **109**, 389–894 (1999).
 42. R. Willett, J.P. Eisenstein, H.L. Stormer, D.C. Tsui, A.C. Gossard, and J.H. English, Observation of an Even-Denominator Quantum Number in the Fractional Quantum Hall Effect, *Phys. Rev. Lett.* **59**, 1776–1779 (1987).
 43. J.P. Eisenstein, R.L. Willett, H.L. Stormer, L.N. Pfeiffer, and K.W. West, Activation Energies for the Even-Denominator Fractional Quantum Hall Effect, *Surf. Sci.* **229**, 31–33 (1990).
 44. W. Pan, J.-S. Xia, V. Shvarts, D.E. Adams, H.L. Stormer, D.C. Tsui, L.N. Pfeiffer, K.W. Baldwin, and K.W. West, Exact Quantization of the Even-Denominator Fractional Quantum Hall State at $\nu = 5/2$ Landau Level Filling Factor, *Phys. Rev. Lett.* **83**, 3530–3533 (1999).
 45. J.P. Eisenstein, K.B. Cooper, L.N. Pfeiffer, and K.W. West, Insulating and Fractional Quantum Hall States in the First Excited Landau Level, *Phys. Rev. Lett.* **88**, 076801 (2002).
 46. J.S. Xia, W. Pan, C.L. Vicente, E.D. Adams, N.S. Sullivan, H.L. Stormer, D.C. Tsui, L.N. Pfeiffer, K.W. Baldwin, and K.W. West, Electron Correlation in the Second Landau Level: A Competition Between Many Nearly Degenerate Quantum Phases, *Phys. Rev. Lett.* **93**, 176809 (2004).
 47. J.S. Xia, E.D. Adams, V. Shvarts, W. Pan, H.L. Stormer, and D.C. Tsui, Ultra-low-temperature Cooling of Two-Dimensional Electron Gas, *Physica B* **280**, 491–492 (2000).
 48. J. Huang, J.S. Xia, D.C. Tsui, L.N. Pfeiffer, and K.W. West, Disappearance of Metal-Like Behavior in GaAs Two-Dimensional Holes below 30 mK, *Phys. Rev. Lett.* **98**, 226801 (2007).
 49. W. Li, C.L. Vicente, J.S. Xia, W. Pan, D.C. Tsui, L.N. Pfeiffer, and K.W. West, Scaling in Plateau-to-Plateau Transition: A Direct Connection of Quantum Hall Systems with the Anderson Localization Model, *Phys. Rev. Lett.* **102**, 216801 (2009).
 50. J.S. Xia, E.D. Adams, N.S. Sullivan, W. Pan, H.L. Stormer, and D.C. Tsui, Sample Cooling and Rotation at Ultra-Low Temperatures and High Magnetic Fields, *International Journal of Modern Physics B* **16**, 2986–2989 (2002).
 51. A.C. Clark, K.K. Schwarzwälder, T. Bandi, D. Maradan, and D.M. Zumbühl, Method for Cooling Nanostructures to Microkelvin Temperatures, *Rev. Sci. Instrum.* **81**, 103904 (2010).
 52. M. Palma, D. Maradan, L. Casparis, T.-M. Liu, N.M. Froning, and D.M. Zumbühl, Magnetic Cooling for Microkelvin Nanoelectronics on a Cryofree Platform, *Rev. Sci.*

- Instrum.* **88**, 043902 (2017).
53. D.I. Bradley, A.M. Guénault, D. Gunnarsson, R.P. Haley, S. Holt, A.T. Jones, Yu.A. Pashkin, J. Penttilä, J.R. Prance, M. Prunnila, and L. Roschier, On-chip Magnetic Cooling of a Nanoelectronic Device, *Scientific Reports* **7**, 45566 (2017).
 54. N. Yurttagül, M. Sarsby, and A. Geresdi, Indium as a High Cooling Power Nuclear Refrigerant for Quantum Nanoelectronics, *Phys. Rev. Applied* **12**, 011005 (2019).
 55. N. Samkharadze, A. Kumar, M.J. Manfra, L.N. Pfeiffer, K.W. West and G.A. Csáthy, Integrated Electronic Transport and Thermometry at milliKelvin Temperatures and in Strong Magnetic Fields, *Rev. Sci. Instrum.* **82** 053902 (2011).
 56. N. Samkharadze, A. Kumar, and G.A. Csáthy, A New Type of Carbon Resistance Thermometer with Excellent Thermal Contact at Millikelvin Temperatures, *J. Low Temp. Phys.* **160**, 246–253 (2010).
 57. A. Shibahara, O. Hahtela, J. Engert, H. van der Vliet, L.V. Levitin, A. Casey, C.P. Lusher, J. Saunders, D. Drung, and Th. Schurig, Primary Current-Sensing Noise Thermometry in the Millikelvin Regime, *Phil. Trans. Royal Soc. A* **374**, 20150054 (2016).
 58. E. Kleinbaum, V. Shingla, and G.A. Csáthy, SQUID-Based Current Sensing Noise Thermometry for Quantum Resistors at Dilution Refrigerator Temperatures, *Rev. Sci. Instrum.* **88**, 034902 (2017).
 59. Z. Iftikhar, A. Anthore, S. Jezouin, F.D. Parmentier, Y. Jin, A. Cavanna, A. Ouerghi, U. Gennse, and F. Pierre, Primary Thermometry Triad at 6 mK in Mesoscopic Circuits, *Nature Commun.* **7**, 12908 (2016).
 60. D. Maradan, L. Casparis, T.-M. Liu, D.E.F. Biesinger, C.P. Scheller, D.M. Zumbühl, J.D. Zimmerman, and A.C. Gossard, GaAs Quantum Dot Thermometry Using Direct Transport and Charge Sensing, *J. Low Temp. Phys.* **175**, 784–798 (2014).
 61. A.V. Feshchenko, L. Casparis, I.M. Khaymovich, D. Maradan, O.-P. Saira, M. Palma, M. Meschke, J.P. Pekola, and D.M. Zumbühl, Tunnel-Junction Thermometry Down to Millikelvin Temperatures, *Phys. Rev. Appl.* **4**, 034001 (2015).
 62. D.I. Bradley, R.E. George, D. Gunnarsson, R.P. Haley, H. Heikkinen, Yu.A. Pashkin, J. Penttilä, J.R. Prance, M. Prunnila, L. Roschier, and M. Sarsby, Nanoelectronic Primary Thermometry below 4 mK, *Nature Commun.* **7**, 10455 (2016).
 63. M. Palma, C.P. Scheller, D. Maradan, A.V. Feshchenko, M. Meschke, and D.M. Zumbühl, On-and-off Chip Cooling of a Coulomb Blockade Thermometer down to 2.8 mK, *Appl. Phys. Lett.* **111**, 253105 (2017).
 64. H.L. Störmer, R. Dingle, A.C. Gossard, W. Wiegmann, and M.D. Sturge, Two-Dimensional Electron Gas at a Semiconductor-Semiconductor Interface, *Solid State Commun.* **29**, 707–709 (1979).
 65. H.L. Störmer, A.C. Gossard, W. Wiegmann, and K. Baldwin, Dependence of Electron Mobility in Modulation-Doped GaAs-(AlGa)As Heterojunction Interfaces on Electron Density and Al Concentration, *Appl. Phys. Lett.* **39**, 912–915 (1981).
 66. M. Samani, A.V. Rossokhaty, E. Sajadi, S. Lüscher, J.A. Folk, J.D. Watson, G.C. Gardner, and M.J. Manfra, Low-Temperature Illumination and Annealing of Ultrahigh Quality Quantum Wells, *Phys. Rev. B* **90**, 121405 (2014).
 67. J. Shabani, Y. Liu, and M. Shayegan, Fractional Quantum Hall Effect at High Fillings in a Two-Subband Electron System, *Phys. Rev. Lett.* **105**, 246805 (2010).
 68. Y. Liu, D. Kamburov, M. Shayegan, L.N. Pfeiffer, K.W. West, and K.W. Baldwin, Anomalous Robustness of the $\nu = 5/2$ Fractional Quantum Hall State near a Sharp Phase Boundary, *Phys. Rev. Lett.* **107**, 176805 (2011).
 69. Z. Papić, F.D.M. Haldane, and E.H. Rezayi, Quantum Phase Transitions and the $\nu = 5/2$ Fractional Hall State in Wide Quantum Wells, *Phys. Rev. Lett.* **109**, 266806 (2012).

70. A. Kumar, G.A. Csáthy, M.J. Manfra, L.N. Pfeiffer, and K.W. West, Nonconventional Odd-Denominator Fractional Quantum Hall States in the Second Landau Level, *Phys. Rev. Lett.* **105**, 246808 (2010).
71. E. Kleinbaum, A. Kumar, L.N. Pfeiffer, K.W. West, and G.A. Csáthy, Gap Reversal at Filling Factors $3 + 1/3$ and $3 + 1/5$: Towards Novel Topological Order in the Fractional Quantum Hall Regime, *Phys. Rev. Lett.* **114**, 076801 (2015).
72. W. Pan, J.S. Xia, H.L. Stormer, D.C. Tsui, C.L. Vicente, E.D. Adams, N.S. Sullivan, L.N. Pfeiffer, K.W. Baldwin, and K.W. West, Quantization of the Diagonal Resistance: Density Gradients and the Empirical Resistance Rule in a 2D System, *Phys. Rev. Lett.* **95**, 066808 (2005).
73. Q. Qian, J. Nakamura, S. Fallahi, G.C. Gardner, J.D. Watson, S. Lüscher, J.A. Folk, G.A. Csáthy, and M.J. Manfra, Quantum Lifetime in Ultrahigh Quality GaAs Quantum Wells: Relationship to $\Delta_{5/2}$ and Impact of Density Fluctuations, *Phys. Rev. B* **96**, 035309 (2017).
74. D. Kamburov, K.W. Baldwin, K.W. West, S. Lyon, L.N. Pfeiffer, and A. Pinczuk, Use of Micro-Photoluminescence as a Contactless Measure of the 2D Electron Density in a GaAs Quantum Well, *Appl. Phys. Lett.* **110**, 262104 (2017).
75. Y.J. Chung, K.W. Baldwin, K.W. West, N. Haug, J. van de Wetering, M. Shayegan, and L.N. Pfeiffer, Spatial Mapping of Local Density Variations in Two-dimensional Electron Systems Using Scanning Photoluminescence, *Nano Lett.* **19**, 1908–1913 (2019).
76. A. Wójs, Transition from Abelian to non-Abelian Quantum Liquids in the Second Landau Level, *Phys. Rev. B* **80**, 041104 (2009).
77. S.H. Simon, E.H. Rezayi, N.R. Cooper, and I. Berdnikov, Construction of a Paired Wave Function for Spinless Electrons at Filling Fraction $\nu = 2/5$, *Phys. Rev. B* **75**, 075317 (2007).
78. W. Bishara, G.A. Fiete, and C. Nayak, Quantum Hall States at $\nu = 2/(k+2)$: Analysis of the Particle-Hole Conjugates of the General Level- k Read-Rezayi States, *Phys. Rev. B* **77**, 241306 (2008).
79. P. Bonderson and J.K. Slingerland, Fractional Quantum Hall Hierarchy and the Second Landau Level, *Phys. Rev. B* **78**, 125323 (2008).
80. B.A. Bernevig and F.D.M. Haldane, Properties of Non-Abelian Fractional Quantum Hall States at Filling $\nu = k/r$, *Phys. Rev. Lett.* **101**, 246806 (2008).
81. M. Levin and B.I. Halperin, Collective States of Non-Abelian Quasiparticles in a Magnetic Field, *Phys. Rev. B* **79**, 205301 (2009).
82. G.J. Sreejith, C. Tóke, A. Wójs, and J. K. Jain, Bipartite Composite Fermion States, *Phys. Rev. Lett.* **107**, 086806 (2011).
83. G.J. Sreejith, Y.-H. Wu, A. Wójs, and J.K. Jain, Tripartite Composite Fermion States, *Phys. Rev. B* **87**, 245125 (2013).
84. N. d’Ambrumenil and A.M. Reynolds, Fractional Quantum Hall States in Higher Landau Levels, *J. Phys. C* **21**, 119–132 (1988).
85. V.W. Scarola and J.K. Jain, Phase Diagram of Bilayer Composite Fermion States, *Phys. Rev. B* **64**, 085313 (2001).
86. C. Tóke, M.R. Peterson, G.S. Jeon, and J.K. Jain, Fractional Quantum Hall Effect in the Second Landau Level: The Importance of Inter-Composite-Fermion Interaction, *Phys. Rev. B* **72**, 125315 (2005).
87. Z. Papić, N. Regnault, and S. Das Sarma, Interaction-Tuned Compressible-to-Incompressible Phase Transitions in Quantum Hall Systems, *Phys. Rev. B* **80**, 201303 (2009).
88. A.C. Balram, Y.-H. Wu, G.J. Sreejith, A. Wójs, and J.K. Jain, Role of Exciton Screening in the $7/3$ Fractional Quantum Hall Effect, *Phys. Rev. Lett.* **110**, 186801

- (2013).
89. S. Johri, Z. Papić, R.N. Bhatt, and P. Schmitteckert, Quasiholes of $1/3$ and $7/3$ Quantum Hall States: Size Estimates via Exact Diagonalization and Density-Matrix Renormalization Group, *Phys. Rev. B* **89**, 115124 (2014).
 90. M.R. Peterson, Y.-L. Wu, M. Cheng, M. Barkeshli, Z. Wang, and S. Das Sarma, Abelian and Non-Abelian States in $\nu = 2/3$ Bilayer Fractional Quantum Hall Systems, *Phys. Rev. B* **92**, 035103 (2015).
 91. T. Jolicoeur, Shape of the Magnetoroton at $\nu = 1/3$ and $\nu = 7/3$ in Real Samples, *Phys. Rev. B* **95**, 075201 (2017).
 92. J.-S. Jeong, H. Lu, K.H. Lee, K. Hashimoto, S.B. Chung, and K Park, Competing States for the Fractional Quantum Hall Effect in the $1/3$ -Filled Second Landau Level, *Phys. Rev. B* **96**, 125148 (2017).
 93. W. Pan, J.S. Xia, H.L. Stormer, D.C. Tsui, C. Vicente, E.D. Adams, N.S. Sullivan, L.N. Pfeiffer, K.W. Baldwin, and K.W. West, Experimental Studies of the Fractional Quantum Hall Effect in the First Excited Landau Level, *Phys. Rev. B* **77**, 075307 (2008).
 94. C. Zhang, C. Huan, J.S. Xia, N.S. Sullivan, W. Pan, K.W. Baldwin, K.W. West, L.N. Pfeiffer, and D.C. Tsui, Spin Polarization of the $\nu = 12/5$ Fractional Quantum Hall State, *Phys. Rev. B* **85**, 241302 (2012).
 95. N. Deng, J.D. Watson, L.P. Rokhinson, M.J. Manfra, and G.A. Csáthy, Contrasting Energy Scales of Reentrant Integer Quantum Hall States, *Phys. Rev. B* **86**, 201301 (2012).
 96. Q. Qian, J. Nakamura, S. Fallahi, G.C. Gardner, and M.J. Manfra, Possible Nematic to Smectic Phase Transition in a Two-Dimensional Electron Gas at Half-Filling, *Nat. Commun.* **8**, 1536 (2017).
 97. V. Shingla, E. Kleinbaum, A. Kumar, L.N. Pfeiffer, K.W. West, and G.A. Csáthy, Finite-Temperature Behavior in the Second Landau Level of the Two-Dimensional Electron Gas, *Phys. Rev. B* **97**, 241105 (2018).
 98. H.C. Choi, W. Kang, S. Das Sarma, L.N. Pfeiffer, and K.W. West, Activation Gaps of Fractional Quantum Hall Effect in the Second Landau Level, *Phys. Rev. B* **77**, 081301 (2008).
 99. G.S. Boebinger, H.L. Stormer, D.C. Tsui, A.M. Chang, J.C.M. Hwang, A.Y. Cho, C.W. Tu, and G. Weimann, Activation Energies and Localization in the Fractional Quantum Hall Effect, *Phys. Rev. B* **36**, 7919–29 (1987).
 100. R.L. Willett, H.L. Stormer, D.C. Tsui, A.C. Gossard, and J.H. English, Quantitative Experimental Test for the Theoretical Gap Energies in the Fractional Quantum Hall Effect, *Phys. Rev. B* **37**, 8476–8479 (1988).
 101. R.R. Du, H.L. Stormer, D.C. Tsui, L.N. Pfeiffer, and K.W. West, Experimental Evidence for New Particles in the Fractional Quantum Hall Effect, *Phys. Rev. Lett.* **70**, 2944–2947 (1993).
 102. H.C. Manoharan, M. Shayegan, and S.J. Klepper, Signatures of a Novel Fermi Liquid in a Two-Dimensional Composite Particle Metal, *Phys. Rev. Lett.* **73**, 3270–3773 (1994).
 103. M. Dolev, Y. Gross, R. Sabo, I. Gurman, M. Heiblum, V. Umansky, and D. Mahalu, Characterizing Neutral Modes of Fractional States in the Second Landau Level, *Phys. Rev. Lett.* **107**, 036805 (2011).
 104. S. Baer, C. Rössler, T. Ihn, K. Ensslin, C. Reichl, and W. Wegscheider, Experimental Probe of Topological Orders and Edge Excitations in the Second Landau Level, *Phys. Rev. B* **90**, 075403 (2014).
 105. U. Wurstbauer, A.L. Levy, A. Pinczuk, K.W. West, L.N. Pfeiffer, M.J. Manfra, G.C. Gardner, and J.D. Watson, Gapped Excitations of Unconventional Fractional Quantum

- Hall Effect States in the Second Landau Level, *Phys. Rev. B* **92**, 241407 (2015).
106. A.C. Balram, S. Mukherjee, K. Park, M. Barkeshli, M.S. Rudner, and J.K. Jain, Fractional Quantum Hall Effect at $\nu = 2 + 6/13$: The Parton Paradigm for the Second Landau Level, *Phys. Rev. Lett.* **121**, 186601 (2018).
 107. A.C. Balram, M. Barkeshli, and M.S. Rudner, Parton Construction of a Wave Function in the Anti-Pfaffian Phase, *Phys. Rev. B* **98**, 035127 (2018).
 108. A.C. Balram, M. Barkeshli, and M.S. Rudner, Parton Construction of Particle-Hole-Conjugate Read-Rezayi Parafermion Fractional Quantum Hall States and Beyond, *Phys. Rev. B* **99**, 241108 (2019).
 109. E.H. Rezayi and N. Read, Non-Abelian Quantized Hall States of Electrons at Filling Factors $12/5$ and $13/5$ in the First Excited Landau Level, *Phys. Rev. B* **79**, 075306 (2009).
 110. W. Zhu, S.S. Gong, F.D.M. Haldane, and D.N. Sheng, Fractional Quantum Hall States at $\nu = 13/5$ and $12/5$ and Their Non-Abelian Nature, *Phys. Rev. Lett.* **115**, 126805 (2015).
 111. K. Pakrouski, M. Troyer, Y.-L. Wu, S. Das Sarma, and M.R. Peterson, Enigmatic $12/5$ Fractional Quantum Hall Effect, *Phys. Rev. B* **94**, 075108 (2016).
 112. R.S.K. Mong, M.P. Zaletel, F. Pollmann, and Z. Papić, Fibonacci Anyons and Charge Density Order in the $12/5$ and $13/5$ Quantum Hall Plateaus, *Phys. Rev. B* **95**, 115136 (2017).
 113. P. Bonderson, A.E. Feiguin, G. Möller, and J.K. Slingerland, Competing Topological Orders in the $\nu = 12/5$ Quantum Hall State, *Phys. Rev. Lett.* **108**, 036806 (2012).
 114. A.A. Zibrov, C. Kometter, H. Zhou, E.M. Spanton, T. Taniguchi, K. Watanabe, M.P. Zaletel, and A.F. Young, Tunable Interacting Composite Fermion Phases in a Half-Filled Bilayer-Graphene Landau Level, *Nature* **549** 360–364, (2017).
 115. W. Pan, K.W. Baldwin, K.W. West, L.N. Pfeiffer, and D.C. Tsui, Spin Transition in the $\nu = 8/3$ Fractional Quantum Hall Effect, *Phys. Rev. Lett.* **108**, 216804 (2012).
 116. D.M. Haldane, E.H. Rezayi, and K. Yang, Spontaneous Breakdown of Translational Symmetry in Quantum Hall Systems: Crystalline Order in High Landau Levels, *Phys. Rev. Lett.* **85**, 5396–5399 (2000).
 117. N. Shibata and D. Yoshioka, Ground-State Phase Diagram of 2D Electrons in a High Landau Level: A Density-Matrix Renormalization Group Study, *Phys. Rev. Lett.* **86**, 5755–5758 (2001).
 118. C.R. Dean, B.A. Piot, P. Hayden, S. Das Sarma, G. Gervais, L.N. Pfeiffer, and K.W. West, Intrinsic Gap of the $\nu = 5/2$ Fractional Quantum Hall State, *Phys. Rev. Lett.* **100**, 146803 (2008).
 119. J. Nuebler, V. Umansky, R. Morf, M. Heiblum, K. von Klitzing, and J. Smet, Density Dependence of the $\nu = 5/2$ Energy Gap: Experiment and Theory, *Phys. Rev. B* **81**, 035316 (2010).
 120. J.R. Mallett, R.G. Clark, R.J. Nicholas, R. Willett, J.J. Harris, and C.T. Foxon, Experimental Studies of the $\nu = 1/5$ Hierarchy in the Fractional Quantum Hall Effect, *Phys. Rev. B* **38**, 2200–2203 (1988).
 121. W. Pan, H.L. Stormer, D.C. Tsui, L.N. Pfeiffer, K.W. Baldwin, and K.W. West, Fractional Quantum Hall Effect of Composite Fermions, *Phys. Rev. Lett.* **90**, 016801 (2003).
 122. P. Sitko, K.-S. Yi, and J.J. Quinn, Composite Fermion Hierarchy: Condensed States of Composite Fermion Excitations, *Phys. Rev. B* **56**, 12417 (1997).
 123. A. Wójs, K.-S. Yi, J.J. Quinn, Fractional Quantum Hall States of Clustered Composite Fermions, *Phys. Rev. B* **69**, 205322 (2004).
 124. A. Wójs, G. Simion, and J.J. Quinn, Spin Phase Diagram of the $\nu_e = 4/11$ Composite

- Fermion Liquid, *Phys. Rev. B* **75**, 155318 (2007).
125. S. Mukherjee, S.S. Mandal, Y.-H. Wu, A. Wójs, and J. K. Jain, Enigmatic $4/11$ State: A Prototype for Unconventional Fractional Quantum Hall Effect, *Phys. Rev. Lett.* **112**, 016801 (2014).
 126. A.C. Balram, Interacting Composite Fermions: Nature of the $4/5$, $5/7$, $6/7$, and $6/17$ Fractional Quantum Hall States, *Phys. Rev. B* **94**, 165303 (2016).
 127. W. Pan, K.W. Baldwin, K.W. West, L.N. Pfeiffer, and D.C. Tsui, Fractional Quantum Hall Effect at Landau Level Filling $\nu = 4/11$, *Phys. Rev. B* **91**, 041301 (2015).
 128. N. Samkharadze, I. Arnold, L.N. Pfeiffer, K.W. West, and G.A. Csáthy, Observation of Incompressibility at $\nu = 4/11$ and $\nu = 5/13$, *Phys. Rev. B* **91**, 081109 (2015).
 129. J. Falson, D. Maryenko, B. Friess, D. Zhang, Y. Kozuka, A. Tsukazaki, J.H. Smet, and M. Kawasaki, Even-Denominator Fractional Quantum Hall Physics in ZnO, *Nature Physics* **11**, 347–351 (2015).
 130. D.-K. Ki, V.I. Falko, D.A. Abanin, and A.F. Morpurgo, Observation of Even Denominator Fractional Quantum Hall Effect in Suspended Bilayer Graphene, *Nano Lett.* **14**, 2135–2139 (2014).
 131. Y. Kim, D.S. Lee, S. Jung, V. Skákalová, T. Taniguchi, K. Watanabe, J.S. Kim, and J.H. Smet, Fractional Quantum Hall States in Bilayer Graphene Probed by Transconductance Fluctuations, *Nano Lett.* **15**, 7445–7451 (2015).
 132. J.I.A. Li, C. Tan, S. Chen, Y. Zeng, T. Taniguchi, K. Watanabe, J. Hone, and C.R. Dean, Even-Denominator Fractional Quantum Hall States in Bilayer Graphene, *Science* **358**, 648–652 (2017).
 133. A.A. Zibrov, E.M. Spanton, H. Zhou, C. Kometter, T. Taniguchi, K. Watanabe, and A.F. Young, Even-Denominator Fractional Quantum Hall States at an Isospin Transition in Monolayer Graphene, *Nature Physics* **14**, 930–935 (2018).
 134. Y. Kim, A.C. Balram, T. Taniguchi, K. Watanabe, J.K. Jain, and J.H. Smet, Even Denominator Fractional Quantum Hall States in Higher Landau Levels of Graphene, *Nature Physics* **15**, 154–158 (2019).
 135. M. Greiter, X.-G. Wen, and F. Wilczek, Paired Hall State at Half Filling, *Phys. Rev. Lett.* **66**, 3205–3208 (1991).
 136. N. Read and D. Green, Paired States of Fermions in Two Dimensions with Breaking of Parity and Time-Reversal Symmetries and the Fractional Quantum Hall Effect, *Phys. Rev. B* **61**, 10267–10297 (2000).
 137. V.W. Scarola, K. Park, and J.K. Jain, Cooper Instability of Composite Fermions, *Nature* **406**, 863–865 (2000).
 138. E.H. Rezayi and F.D.M. Haldane, Incompressible Paired Hall State, Stripe Order, and the Composite Fermion Liquid Phase in Half-Filled Landau Levels, *Phys. Rev. Lett.* **84**, 4685–4688 (2000).
 139. H. Lu, S. Das Sarma, and K. Park, Superconducting Order Parameter for the Even-Denominator Fractional Quantum Hall Effect, *Phys. Rev. B* **82**, 201303 (2010).
 140. S.A. Parameswaran, S.A. Kivelson, S.L. Sondhi, and B.Z. Spivak, Weakly Coupled Pfaffian as a Type I Quantum Hall Liquid, *Phys. Rev. Lett.* **106**, 236801 (2011).
 141. M. Levin, B.I. Halperin, and B. Rosenow, Particle-Hole Symmetry and the Pfaffian State, *Phys. Rev. Lett.* **99**, 236806 (2007).
 142. S.-S. Lee, S. Ryu, C. Nayak, and M.P.A. Fisher, Particle-Hole Symmetry and the $\nu = 5/2$ Quantum Hall State, *Phys. Rev. Lett.* **99**, 236807 (2007).
 143. B.I. Halperin, Theory of the Quantized Hall Conductance, *Helv. Phys. Acta* **56**, 75–102 (1983).
 144. J.-S. Jeong and K. Park, Bilayer Mapping of the Paired Quantum Hall State: Instability Toward Anisotropic Pairing, *Phys. Rev. B* **91**, 195119 (2015).

145. D.T. Son, Is the Composite Fermion a Dirac Particle?, *Phys. Rev. X* **5**, 031027 (2015).
146. P.T. Zucker and D.E. Feldman, Stabilization of the Particle-Hole Pfaffian Order by Landau-Level Mixing and Impurities That Break Particle-Hole Symmetry, *Phys. Rev. Lett.* **117**, 096802 (2016).
147. X. Wan and Kun Yang, Striped Quantum Hall State in a Half-Filled Landau Level, *Phys. Rev. B* **93**, 201303 (2016).
148. X.G. Wen and Q. Niu, Ground-State Degeneracy of the Fractional Quantum Hall States in the Presence of a Random Potential and on High-Genus Riemann Surfaces, *Phys. Rev. B* **41**, 9377–9396 (1990).
149. X.G. Wen, Non-Abelian Statistics in the Fractional Quantum Hall States, *Phys. Rev. Lett.* **66**, 802–805 (1991).
150. R.L. Willett, The Quantum Hall Effect at $5/2$ Filling Factor, *Rep. Prog. Phys.* **76**, 076501 (2013).
151. X. Lin, R.R. Du, and X. Xie, Recent Experimental Progress of Fractional Quantum Hall Effect: $5/2$ Filling State and Graphene, *National Science Review* **1**, 564–579 (2014).
152. I.P. Radu, J.B. Miller, C.M. Marcus, M.A. Kastner, L.N. Pfeiffer, and K.W. West, Quasi-Particle Properties from Tunneling in the $\nu = 5/2$ Fractional Quantum Hall State, *Science* **320**, 899–902 (2008).
153. X. Lin, C. Dillard, M.A. Kastner, L.N. Pfeiffer, and K.W. West, Measurements of Quasiparticle Tunneling in the $\nu = 5/2$ Fractional Quantum Hall State, *Phys. Rev. B* **85**, 165321 (2012).
154. H. Fu, P. Wang, P. Shan, L.N. Pfeiffer, K.W. West, M.A. Kastner, and X. Lin, Competing $\nu = 5/2$ Fractional Quantum Hall States in Confined Geometry, *Proc. Nat. Acad. Sci.* **113**, 12386–12390 (2016).
155. R.L. Willett, C. Nayak, K. Shtengel, L.N. Pfeiffer, and K.W. West, Magnetic-Field-Tuned Aharonov-Bohm Oscillations and Evidence for Non-Abelian Anyons at $\nu = 5/2$, *Phys. Rev. Lett.* **111**, 186401 (2013).
156. M. Banerjee, M. Heiblum, V. Umansky, D.E. Feldman, Y. Oreg, and A. Stern, Observation of Half-Integer Thermal Hall Conductance, *Nature* **559**, 205–210 (2018).
157. B.A. Schmidt, K. Bennaceur, S. Gaucher, G. Gervais, L.N. Pfeiffer, and K.W. West, Specific Heat and Entropy of Fractional Quantum Hall States in the Second Landau Level, *Phys. Rev. B* **95**, 201306 (2017).
158. W. Pan, A. Serafin, J.S. Xia, L. Yin, N.S. Sullivan, K.W. Baldwin, K.W. West, L.N. Pfeiffer, and D.C. Tsui, Competing Quantum Hall Phases in the Second Landau Level in the Low-Density Limit, *Phys. Rev. B* **89**, 241302 (2014).
159. N. Samkharadze, D. Ro, L.N. Pfeiffer, K.W. West, and G.A. Csáthy, Observation of an Anomalous Density-Dependent Energy Gap of the $\nu = 5/2$ Fractional Quantum Hall State in the Low-Density Regime, *Phys. Rev. B* **96**, 085105 (2017).
160. N. Samkharadze, K.A. Schreiber, G.C. Gardner, M.J. Manfra, E. Fradkin, and G.A. Csáthy, Observation of a Transition from a Topologically Ordered to a Spontaneously Broken Symmetry Phase, *Nature Phys.* **12**, 191–195 (2016).
161. K.A. Schreiber, N. Samkharadze, G.C. Gardner, R.R. Biswas, M.J. Manfra, and G.A. Csáthy, Onset of Quantum Criticality in the Topological-to-Nematic Transition in a Two-Dimensional Electron Gas at Filling Factor $\nu = 5/2$, *Phys. Rev. B* **96**, 041107 (2017).
162. K.A. Schreiber, N. Samkharadze, G.C. Gardner, Y. Lyanda-Geller, M.J. Manfra, L.N. Pfeiffer, K.W. West, and G.A. Csáthy, Electron-Electron Interactions and the Paired-to-Nematic Quantum Phase Transition in the Second Landau Level, *Nature*

- Commun.* **9**, 2400 (2018).
163. L. Tiemann, G. Gamez, N. Kumad, and K. Muraki, Unraveling the Spin Polarization of the $\nu = 5/2$ Fractional Quantum Hall State, *Science* **335**, 828–831 (2012).
 164. U. Wurstbauer, K.W. West, L.N. Pfeiffer, and A. Pinczuk, Resonant Inelastic Light Scattering Investigation of Low-Lying Gapped Excitations in the Quantum Fluid at $\nu = 5/2$, *Phys. Rev. Lett.* **110**, 026801 (2013).
 165. A. Wójs and J.J. Quinn, Landau Level Mixing in the $\nu = 5/2$ Fractional Quantum Hall State, *Phys. Rev. B* **74**, 235319 (2006).
 166. M.R. Peterson, Th. Jolicoeur, and S. Das Sarma, Finite-Layer Thickness Stabilizes the Pfaffian State for the $5/2$ Fractional Quantum Hall Effect: Wave Function Overlap and Topological Degeneracy, *Phys. Rev. Lett.* **101**, 016807 (2008).
 167. A. Wójs, C. Tóke, and J.K. Jain, Landau-Level Mixing and the Emergence of Pfaffian Excitations for the $5/2$ Fractional Quantum Hall Effect, *Phys. Rev. Lett.* **105**, 096802 (2010).
 168. E.H. Rezayi and S.H. Simon, Breaking of Particle-Hole Symmetry by Landau Level Mixing in the $\nu = 5/2$ Quantized Hall State, *Phys. Rev. Lett.* **106**, 116801 (2011).
 169. A. Tylan-Tyler and Y. Lyanda-Geller, Phase Diagram and Edge States of the $\nu = 5/2$ Fractional Quantum Hall State with Landau Level Mixing and Finite Well Thickness, *Phys. Rev. B* **91**, 205404 (2015).
 170. M.P. Zaletel, R.S.K. Mong, F. Pollmann, E.H. Rezayi, Infinite Density Matrix Renormalization Group for Multicomponent Quantum Hall Systems, *Phys. Rev. B* **91**, 045115 (2015).
 171. K. Pakrouski, M.R. Peterson, Th. Jolicoeur, V.W. Scarola, C. Nayak, and M. Troyer, Phase Diagram of the $\nu = 5/2$ Fractional Quantum Hall Effect: Effects of Landau-Level Mixing and Nonzero Width, *Phys. Rev. X* **5**, 021004 (2015).
 172. E.H. Rezayi, Landau Level Mixing and the Ground State of the $\nu = 5/2$ Quantum Hall Effect, *Phys. Rev. Lett.* **119**, 026801 (2017).
 173. W. Luo and T. Chakraborty, Pfaffian State in an Electron Gas with Small Landau Level Gaps, *Phys. Rev. B* **96**, 081108 (2017).
 174. Bo Yang, Three-Body Interactions in Generic Fractional Quantum Hall Systems and Impact of Galilean Invariance Breaking, *Phys. Rev. B* **98**, 201101 (2018).
 175. W. Li, G.A. Csáthy, D.C. Tsui, L.N. Pfeiffer, and K.W. West, Scaling and Universality of Integer Quantum Hall Plateau-to-Plateau Transitions, *Phys. Rev. Lett.* **94**, 206807 (2005).
 176. N. Samkharadze, J.D. Watson, G. Gardner, M.J. Manfra, L.N. Pfeiffer, K.W. West, and G.A. Csáthy, Quantitative Analysis of the Disorder Broadening and the Intrinsic Gap for the Fractional Quantum Hall State, *Phys. Rev. B* **84**, 121305 (2011).
 177. W. Pan, N. Masuhara, N.S. Sullivan, K.W. Baldwin, K.W. West, L.N. Pfeiffer, and D.C. Tsui, Impact of Disorder on the $5/2$ Fractional Quantum Hall State, *Phys. Rev. Lett.* **106**, 206806 (2011).
 178. G. Gamez and K. Muraki, $\nu = 5/2$ Fractional Quantum Hall State in Low-Mobility Electron Systems: Different Roles of Disorder, *Phys. Rev. B* **88**, 075308 (2013).
 179. Q. Qian, J. Nakamura, S. Fallahi, G.C. Gardner, J.D. Watson, and M.J. Manfra, High-Temperature Resistivity Measured at $\nu = 5/2$ as a Predictor of the Two-Dimensional Electron Gas Quality in the $N = 1$ Landau Level, *Phys. Rev. B* **95**, 241304 (2017).
 180. R.H. Morf and N. d’Ambrumenil, Disorder in Fractional Quantum Hall States and the Gap at $\nu = 5/2$, *Phys. Rev. B* **68**, 113309 (2003).
 181. R.H. Morf, Transition from Quantum Hall to Compressible States in the Second Landau Level: New Light on the $\nu = 5/2$ Enigma, *Phys. Rev. Lett.* **80**, 1505–1508

- (1998).
182. A.E. Feiguin, E. Rezayi, C. Nayak, and S. Das Sarma, Density Matrix Renormalization Group Study of Incompressible Fractional Quantum Hall States, *Phys. Rev. Lett.* **100**, 166803 (2008).
 183. A. Kumar, N. Samkharadze, G.A. Csáthy, M.J. Manfra, L.N. Pfeiffer, and K.W. West, Particle-Hole Asymmetry of Fractional Quantum Hall States in the Second Landau Level of a Two-Dimensional Hole System, *Phys. Rev. B* **83**, 201305 (2011).
 184. W. Li, G.A. Csáthy, D.C. Tsui, L.N. Pfeiffer, and K.W. West, Direct Observation of Alloy Scattering of Two-Dimensional Electrons in $\text{Al}_x\text{Ga}_{1-x}\text{As}$, *Appl. Phys. Lett.* **83**, 2823–2834 (2003).
 185. G.C. Gardner, J.D. Watson, S. Mondal, N. Deng, G.A. Csáthy, and M.J. Manfra, Growth and Electrical Characterization of $\text{Al}_{0.24}\text{Ga}_{0.76}\text{As}/\text{Al}_x\text{Ga}_{1-x}\text{As}/\text{Al}_{0.24}\text{Ga}_{0.76}\text{As}$ Modulation-Doped Quantum Wells with Extremely Low x , *Appl. Phys. Lett.* **102**, 252103 (2013).
 186. C. Reichl, W. Dietsche, T. Tschirky, T. Hyart, and W. Wegscheider, Mapping an Electron Wave Function by a Local Electron Scattering Probe, *New J. Phys.* **17**, 113048 (2015).
 187. B.-H. Moon, L.W. Engel, D.C. Tsui, L.N. Pfeiffer, and K.W. West, Microwave Pinning Modes near Landau Filling $\nu = 1$ in Two-dimensional Electron Systems with Alloy Disorder, *Phys. Rev. B* **92**, 035121 (2015).
 188. N. Deng, G.C. Gardner, S. Mondal, E. Kleinbaum, M.J. Manfra, and G.A. Csáthy, $\nu = 5/2$ Fractional Quantum Hall State in the Presence of Alloy Disorder, *Phys. Rev. Lett.* **112**, 116804 (2014).
 189. D.N. Sheng, X. Wan, E.H. Rezayi, K. Yang, R.N. Bhatt, and F. D. M. Haldane, Disorder-Driven Collapse of the Mobility Gap and Transition to an Insulator in the Fractional Quantum Hall Effect, *Phys. Rev. Lett.* **90**, 256802 (2003).
 190. X. Wan, D.N. Sheng, E.H. Rezayi, K. Yang, R.N. Bhatt, and F. D. M. Haldane, Mobility Gap in Fractional Quantum Hall Liquids: Effects of Disorder and Layer Thickness, *Phys. Rev. B* **72**, 075325 (2005).
 191. Z. Liu and R.N. Bhatt, Evolution of Quantum Entanglement with Disorder in Fractional Quantum Hall Liquids, *Phys. Rev. B* **96**, 115111 (2017).
 192. Z. Liu and R.N. Bhatt, Quantum Entanglement as a Diagnostic of Phase Transitions in Disordered Fractional Quantum Hall Liquids, *Phys. Rev. Lett.* **117**, 206801 (2016).
 193. B.A. Friedman, Short and Long Ranged Impurities in Fractional Quantum Hall Systems, *Int. J. Mod. Phys. B* **32**, 1850338 (2018).
 194. W. Li, D.R. Luhman, D.C. Tsui, L.N. Pfeiffer, and K.W. West, Observation of Reentrant Phases Induced by Short-Range Disorder in the Lowest Landau Level of $\text{Al}_x\text{Ga}_{1-x}\text{As}/\text{Al}_{0.32}\text{Ga}_{0.68}\text{As}$ Heterostructures, *Phys. Rev. Lett.* **105**, 076803 (2010).
 195. Y. Liu, C.G. Pappas, M. Shayegan, L.N. Pfeiffer, K.W. West, and K.W. Baldwin, Observation of Reentrant Integer Quantum Hall States in the Lowest Landau Level, *Phys. Rev. Lett.* **109**, 036801 (2012).
 196. K.B. Cooper, M.P. Lilly, J.P. Eisenstein, L.N. Pfeiffer, and K.W. West, Insulating Phases of Two-Dimensional Electrons in High Landau Levels: Observation of Sharp Thresholds to Conduction, *Phys. Rev. B* **60**, 11285 (1999).
 197. N. Deng, A. Kumar, M.J. Manfra, L.N. Pfeiffer, K.W. West, and G.A. Csáthy, Collective Nature of the Reentrant Integer Quantum Hall States in the Second Landau Level, *Phys. Rev. Lett.* **108**, 086803 (2012).
 198. R.M. Lewis, P.D. Ye, L.W. Engel, D.C. Tsui, L.N. Pfeiffer, and K.W. West, Microwave Resonance of the Bubble Phases in $1/4$ and $3/4$ Filled High Landau Levels, *Phys. Rev. Lett.* **89**, 136804 (2002).

199. R.M. Lewis, Y. Chen, L.W. Engel, D.C. Tsui, P.D. Ye, L.N. Pfeiffer, and K.W. West, Evidence of a First-Order Phase Transition Between Wigner-Crystal and Bubble Phases of 2D Electrons in Higher Landau Levels, *Phys. Rev. Lett.* **93**, 176808 (2004).
200. R.M. Lewis, Y.P. Chen, L.W. Engel, D.C. Tsui, L.N. Pfeiffer, and K.W. West, Microwave Resonance of the Reentrant Insulating Quantum Hall Phases in the First Excited Landau Level, *Phys. Rev. B* **71**, 081301 (2005).
201. W.E. Chickering, J.P. Eisenstein, L.N. Pfeiffer, and K.W. West, Thermoelectric Response of Fractional Quantized Hall and Reentrant Insulating States in the $N = 1$ Landau level, *Phys. Rev. B* **87**, 075302 (2013).
202. X. Wang, H. Fu, L. Du, X. Liu, P. Wang, L.N. Pfeiffer, K.W. West, R.R. Du, and X. Lin, Depinning transition of bubble phases in a high Landau level, *Phys. Rev. B* **91**, 115301 (2015).
203. S. Baer, C. Rössler, S. Hennel, H.C. Overweg, T. Ihn, K. Ensslin, C. Reichl, and W. Wegscheider, Nonequilibrium Transport in Density-Modulated Phases of the Second Landau Level, *Phys. Rev. B* **91**, 195414 (2015).
204. A.V. Rossokhaty, Y. Baum, J.A. Folk, J.D. Watson, G.C. Gardner, and M.J. Manfra, Electron-Hole Asymmetric Chiral Breakdown of Reentrant Quantum Hall States, *Phys. Rev. Lett.* **117**, 166805 (2016).
205. K. Bennaceur, C. Lupien, B. Reulet, G. Gervais, L.N. Pfeiffer, and K.W. West, Competing Charge Density Waves Probed by Nonlinear Transport and Noise in the Second and Third Landau Levels, *Phys. Rev. Lett.* **120**, 136801 (2018).
206. B. Friess, V. Umansky, K. von Klitzing, and J.H. Smet, Current Flow in the Bubble and Stripe Phases, *Phys. Rev. Lett.* **120**, 137603 (2018).
207. M.E. Msall and W. Dietsche, Acoustic Measurements of the Stripe and the Bubble Quantum Hall Phase, *New J. Phys.* **17**, 043042 (2015).
208. B. Friess, Y. Peng, B. Rosenow, F. von Oppen, V. Umansky, K. von Klitzing, and J.H. Smet, Negative Permittivity in Bubble and Stripe Phases, *Nature Phys.* **13**, 1124–1129 (2017).
209. S. Chen, R. Ribeiro-Palau, K. Yang, K. Watanabe, T. Taniguchi, J. Hone, M.O. Goerbig, and C.R. Dean, Competing Fractional Quantum Hall and Electron Solid Phases in Graphene, *Phys. Rev. Lett.* **122**, 026802 (2019).
210. H.W. Jiang, R.L. Willett, H.L. Stormer, D.C. Tsui, L.N. Pfeiffer, and K.W. West, Quantum Liquid versus Electron Solid around $\nu = 1/5$ Landau-Level Filling, *Phys. Rev. Lett.* **65**, 633–636 (1990).
211. D.K. Maude and J.C. Portal, "Parallel transport in low-dimensional semiconductor structures", in *Semiconductors and Semimetals*. **55**, 1–43 (1998).
212. H. Cho, J.B. Young, W. Kang, K.L. Campman, A.C. Gossard, M. Bichler, and W. Wegscheider, Hysteresis and Spin Transitions in the Fractional Quantum Hall Effect, *Phys. Rev. Lett.* **81**, 2522–2525 (1998).
213. E.H. Rezayi and F.D.M. Haldane, Incompressible Paired Hall State, Stripe Order, and the Composite Fermion Liquid Phase in the Half-Filled Landau Levels, *Phys. Rev. Lett.* **84**, 4685–4688 (2000).
214. W. Pan, R.R. Du, H.L. Stormer, D.C. Tsui, L.N. Pfeiffer, K.W. Baldwin, and K.W. West, Strongly Anisotropic Electronic Transport at Landau Level Filling Factor $\nu = 9/2$ and $\nu = 5/2$ under a Tilted Magnetic Field, *Phys. Rev. Lett.* **83**, 820–823 (1999).
215. M.P. Lilly, K.B. Cooper, J.P. Eisenstein, L.N. Pfeiffer, and K.W. West, Anisotropic States of Two-Dimensional Electron Systems in High Landau Levels: Effect of an In-Plane Magnetic Field, *Phys. Rev. Lett.* **83**, 824–827 (1999).
216. Y. You, G.Y. Cho, and E. Fradkin, Nematic Quantum Phase Transition of Composite Fermi Liquids in Half-Filled Landau Levels and Their Geometric Response. *Phys. Rev.*

- B* **93**, 205401 (2016).
217. A. Zhu, I. Sodemann, D.N. Sheng, and L. Fu, Anisotropy-Driven Transition from the Moore-Read State to Quantum Hall Stripes. *Phys. Rev. B* **95**, 201116 (2017).
218. A. Mesaros, M.J. Lawler, and E.-A. Kim, Nematic Fluctuations Balancing the Zoo of Phases in Half-Filled Quantum Hall Systems, *Phys. Rev. B* **95**, 125127 (2017).
219. K. Lee, J. Shao, E.-A. Kim, F.D.M. Haldane, and E.H. Rezayi, Pomeranchuk Instability of Composite Fermi Liquid. *Phys. Rev. Lett.* **121**, 147601 (2018).
220. D.X. Nguyen, A. Gromov, and D.T. Son, Fractional Quantum Hall Systems near Nematicity: Bimetric Theory, Composite Fermions, and Dirac Brackets, *Phys. Rev. B* **97**, 195103 (2018).
221. L.H. Santos, Y. Wang, and E. Fradkin, Pair-Density-Wave Order and Paired Fractional Quantum Hall Fluids, *Phys. Rev. X* **9**, 021047 (2019).